ISTANBUL TECHNICAL UNIVERSITY ★ GRADUATE SCHOOL

MEASUREMENT-BASED ANTENNA MISALIGNMENT ANALYSIS AND ANGLE OF ARRIVAL ESTIMATION FOR TERAHERTZ WIRELESS COMMUNICATION SYSTEMS

M.Sc. THESIS

Hasan NAYİR

Department of Electronics and Communication Engineering

Telecommunication Engineering Programme

SEPTEMBER 2023

ISTANBUL TECHNICAL UNIVERSITY ★ GRADUATE SCHOOL

MEASUREMENT-BASED ANTENNA MISALIGNMENT ANALYSIS AND ANGLE OF ARRIVAL ESTIMATION FOR TERAHERTZ WIRELESS COMMUNICATION SYSTEMS

M.Sc. THESIS

Hasan NAYİR
(504201323)

Department of Electronics and Communication Engineering

Telecommunication Engineering Programme

Thesis Advisor: Prof. Dr. Güneş Karabulut Kurt

SEPTEMBER 2023

İSTANBUL TEKNİK ÜNİVERSİTESİ ★ LİSANSÜSTÜ EĞİTİM ENSTİTÜSÜ

KABLOSUZ HABERLEŞME SİSTEMLERİNDE ÖLÇÜM TABANLI HATALI ANTEN HİZALAMASI ANALİZİ VE GELİŞ AÇISI KESTİRİMİ

YÜKSEK LİSANS TEZİ

Hasan NAYİR
(504201323)

Elektronik ve Haberleşsme Mühendisliği Anabilim Dalı

Telekomünikasyon Mühendisliği Programı

Tez Danışmanı: Prof. Dr. Güneş Karabulut Kurt

EYLÜL 2023

Hasan NAYİR, a M.Sc. student of ITU Graduate School student ID 504201323 successfully defended the thesis entitled "MEASUREMENT-BASED ANTENNA MISALIGNMENT ANALYSIS AND ANGLE OF ARRIVAL ESTIMATION FOR TERAHERTZ WIRELESS COMMUNICATION SYSTEMS", which he prepared after fulfilling the requirements specified in the associated legislations, before the jury whose signatures are below.

Thesis Advisor :	**Prof. Dr. Güneş Karabulut Kurt** Istanbul Technical University	.....
Jury Members :	**Prof. Dr. Selçuk PAKER** Istanbul Technical University	.....
	Prof. Dr. Berna ÖZBEK İzmir Institute of Technology	.....

Date of Submission : **26 May 2023**
Date of Defense : **7 September 2023**

To my family,

FOREWORD

Throughout this process, I have received invaluable guidance and support from my thesis advisor, Güneş Karabulut Kurt. Their expertise and unwavering commitment to academic excellence have been instrumental in shaping the direction of this thesis. I am deeply grateful for their mentorship and guidance.

I would like to extend my heartfelt appreciation to my colleagues at TÜBİTAK BİLGEM HİSAR Laboratory and my friends for their unwavering support and encouragement. Their belief in my abilities has been a constant source of motivation, and I am grateful for their presence throughout this journey.

Last but not least, I express my gratitude to my parents and sister for their unwavering love and support throughout the years. I am indebted to their blessings and constant encouragement, which have been crucial factors in my achievements.

September 2023

Hasan NAYİR
(Electronics and Communication Engineer)

TABLE OF CONTENTS

ABBREVIATIONS

ABS : Aerial Base Station
AoA : Angle of Arrival
AoSA : Array-of-Subarrays
AWGN : Additive White Gaussian Noise
BFT : Beamforming Training
CFR : Channel Frequency Response
CIR : Channel Impulse Response
CSI : Channel State Information
CS : Compressive Sensing
DoA : Direction-of-Arrival
ESPRIT : Estimation of Signal Parameters via Rotational Invariant Techniques
FC : Fully-Connected
FT : Fourier Transform
IF : Intermediate Frequency
LoS : Line-of-Sight
MIMO : Multiple-Input Multiple-Output
mm-Wave : Millimeter Wave
MUSIC : Multiple Signal Classification
NASA : National Aeronautics and Space Administration
NLoS : Non-Line-of-Sight
OML : Oleson Microwave Labs
RF : Radio Frequency
RMSE : Root Mean Square Error
SIN : Space Information Network
SNR : Signal-to-Noise Ratio
TÜBITAK : Scientific and Technological Research Council of Turkey
THz : Terahertz
UAV : Unmanned Aerial Vehicles
UM-MIMO : Ultra Massive Multiple-Input Multiple-Output
UPA : Uniform Planar Array
VNA : Vector Network Analyzer

SYMBOLS

f_c	: Carrier frequency
x_I	: In-phase component
x_Q	: Quadrature component
L	: Number of multipath components
α_l	: Channel complex gain for the l-th path
t_l	: Delay for the l-th path
α_f	: LoS path complex gain
θ	: Phase of the signal
t_0	: Propagation delay
d	: Distance between transmitter and receiver
c	: Speed of the light
P_{ref}	: Path loss at a reference point
n	: Path loss exponent
M	: Antenna misalignment factor
N_x	: Number of antenna elements in x-axes
N_z	: Number of antenna elements in z-axes
α	: Complex path gain
ε	: Residual Doppler
ϕ	: Azimuth angle
θ	: Elevation angle
a_{RX}	: Array steering vector of the receiver
a_{TX}	: Array steering vector of the transmitter
n_x	: Index of the antenna elements in x-axes
n_z	: Index of the antenna elements in z-axes
λ	: Wavelength
N_{RF}	: Number of RF-chains
N_A	: Number of antennas
N_S	: Number of antennas in each subarray
F_c	: Analog precoding matrices
W	: Analog combining matrices
P	: Pilot symbol matrix
ω	: Phase shift coefficient

LIST OF TABLES

LIST OF FIGURES

Page

MEASUREMENT-BASED ANTENNA MISALIGNMENT ANALYSIS AND ANGLE OF ARRIVAL ESTIMATION FOR TERAHERTZ WIRELESS COMMUNICATION SYSTEMS

SUMMARY

As the demand for instant information and faster data transmission rates increases, the bandwidth requirements of wireless communication systems are predicted to exceed the capabilities of current millimeter-wave (mm-Wave) systems. To address this need, Terahertz (THz) wireless communication systems have emerged as a promising option for 6G and future wireless systems, offering a large contiguous bandwidth in the range of 0.1 THz - 10 THz that is applicable for both indoor and outdoor communication. However, the implementation of THz communication systems presents challenges due to substantial propagation losses, molecular absorption, and the effects of antenna misalignment on system performance.

This master's thesis focuses on addressing the aforementioned challenges in THz communication systems. Our primary objective is to analyze the effects of antenna misalignment on system performance. To achieve this, we have designed and implemented a comprehensive measurement system capable of accurately characterizing the impact of misalignment on THz communication channels. By conducting extensive experiments and measurements, we aim to quantify the degradation in system performance caused by antenna misalignment and establish a thorough understanding of the underlying mechanisms. Furthermore, we aim to develop novel angle of arrival (AoA) estimation techniques specifically tailored for THz communication systems. These techniques will leverage advanced signal processing algorithms and innovative antenna array designs to accurately estimate the arrival angles of incoming signals, even in the presence of misalignment. By improving the accuracy of AoA estimation, we anticipate significant advancements in beamforming, spatial multiplexing, and other key aspects of THz system design.

Through our research efforts, we strive to contribute to the development of more efficient and reliable THz wireless communication systems for future generations. By mitigating the impact of antenna misalignment and enhancing the accuracy of AoA estimation, we envision THz systems that can achieve higher data rates, improved coverage, and enhanced overall system performance. This work has the potential to revolutionize wireless communication and pave the way for the seamless integration of THz technology into various applications, including 6G networks, ultra-fast wireless links, and high-capacity communication systems.

As a result, this master's thesis examines the potential of the THz band for wireless communication systems in the face of growing demand for data capacity in mobile networks. The study highlights the limitations of conventional frequency spectrums, such as the mm-Wave systems, and demonstrates how the THz band

can overcome these limitations. The importance of comprehensive measurement campaigns and new algorithms to estimate the AoA and address antenna misalignment in THz wireless communication systems is emphasized. The thesis proposes a new algorithm, the AoSA-gold-MUSIC, which is designed specifically for THz-enabled space information networks (SINs) and is able to estimate AoA accurately while being computationally efficient. The analysis of channel impulse and frequency responses from the measurement campaign provides valuable insights into the behavior of electromagnetic waves in different scenarios and shows how the THz band could pave the way for next-generation wireless communication systems with disruptive metrics. These metrics include data rates of up to 100 Gbps, latency as low as 0.1 ms, and high spectrum efficiency. The thesis underscores the need for further research and development in the THz band and wireless communication systems to unlock its full potential and meet the ever-increasing demand for data capacity and exchange of information.

In Chapter 2, an overview of the issues related to antenna misalignment in THz frequencies and the use of AoA estimation techniques as a potential solution is provided. In particular, the importance of antenna misalignment in THz frequencies, especially in the context unmanned aerial vehicles (UAVs) and SINs that are planned to use THz frequencies is highlighted. Also, the relevance of AoA estimation techniques in addressing the misalignment problem, specifically in the context of SINs that use THz frequencies is discussed in this part of thesis.

In Chapter 3, in order to evaluate the impact of misalignment on THz communication systems, a measurement setup is constructed in the MİILTAL facility located at the Scientific and Technological Research Council of Turkey (TÜBİTAK) in Gebze, Turkey. The setup is designed to model THz channels in the frequency range between 240 GHz and 300 GHz, and a signal model is defined to account for distance-dependent path loss and the potential effects of misalignment. Measurements are being conducted across a range of distances and angles using frequencies ranging from 240 GHz to 300 GHz. The distance intervals are ranged from 20 cm to 100 cm with 10 cm increments. The angle intervals are measured at every distance from 0° to 30°, with 1° intervals from 0° to 15° , and 5° intervals from 15° to 20°. Valuable insights into the behavior of electromagnetic waves in various scenarios is provided by this comprehensive data set. The measurement campaign aim to investigate the impact of varying distances and antenna misalignment on the channel frequency and impulse response within this frequency range. The results of the study show that antenna misalignment is a critical factor for THz wireless communication, with received power being significantly affected by both the distance between antennas and the degree of misalignment. These findings highlight the importance of precise antenna alignment in the design and deployment of THz wireless communication systems.

In Chapter 4, a new method has been introduced to determine the AoA in THz wireless systems with improved accuracy and reduced complexity. The chapter begins by analyzing the channel model, which accounts for residual Doppler in systems that use a uniform planar array (UPA) at both the transmitter and receiver. Then, the array-of-subarrays (AoSA) architecture is used to describe the overall system model for THz communication systems. The AoSA architecture is a commonly

used technique in array signal processing, which divides a large array into smaller subarrays to simplify the processing complexity. Finally, the results indicate that the AoSA-gold-MUSIC algorithm outperforms the standard MUSIC algorithm in terms of computational efficiency. Moreover, the performance of the AoSA-gold-MUSIC algorithm is evaluated for different signal-to-noise ratio (SNR) values and varying residual Doppler variance. This approach can have significant practical implications for THz wireless communication systems.

This thesis explores the potential of the THz band for wireless communication systems, specifically addressing the increasing demand for data capacity in mobile networks. It highlights the limitations of conventional frequency spectrums, such as mmWave systems, and demonstrates how the THz band can overcome these limitations. The thesis emphasizes the importance of comprehensive measurement campaigns and novel algorithms for accurate AoA estimation and addressing antenna misalignment in THz wireless communication systems. It proposes a new algorithm, AoSA-gold-MUSIC, designed specifically for THz-enabled SINs, which offers efficient and accurate AoA estimation. The analysis of channel impulse and frequency responses provides valuable insights into the behavior of electromagnetic waves in different scenarios, showcasing the disruptive potential of the THz band for next-generation wireless communication systems. The thesis concludes by emphasizing the need for further research and development in the THz band and wireless communication systems to unlock its full potential and meet the ever-increasing demand for data capacity and information exchange.

KABLOSUZ HABERLEŞME SİSTEMLERİNDE ÖLÇÜM TABANLI HATALI ANTEN HİZALAMASI ANALİZİ VE GELİŞ AÇISI KESTİRİMİ

ÖZET

Anlık bilgi talepleri ve daha hızlı veri iletim hızlarına olan ihtiyaç arttıkça, kablosuz iletişim sistemlerinin bant genişliği gereksinimlerinin mevcut milimetre dalga (mm-Dalga) sistemlerinin kapasitelerini aşacağı öngörülmektedir. Bu ihtiyaca yanıt olarak, Terahertz (THz) kablosuz iletişim sistemleri, 6G ve gelecekteki kablosuz sistemler için umut vaat eden bir seçenek olarak ortaya çıkmıştır. Hem iç mekan hem de dış mekan iletişimi için uygulanabilen, 0.1 THz - 10 THz aralığında büyük bir sürekli bant genişliği sunmaktadır. Bununla birlikte, THz iletişim sistemlerinin uygulanması, önemli yayılma kayıpları, moleküler emilim ve anten hizalamasının sistem performansı üzerindeki etkileri gibi zorlukları beraberinde getirmektedir.

Elde edilebilen yüksek veri hızları sayesinde, THz bandı birçok farklı sektörde pratikte kullanılabilir hale gelmektedir. Örneğin, tıp sektöründe, THz teknolojisi sayesinde daha hassas teşhis yöntemleri geliştirilebilir. Bu yöntemler, kanser gibi hastalıkların daha erken teşhis edilmesini ve tedavi edilmesini sağlayabilir. Savunma sektöründe ise, THz teknolojisi sayesinde, gizli nesnelerin tespiti ve izlenmesi daha etkili bir şekilde gerçekleştirilebilir. Uzay araştırmaları alanında ise, THz teknolojisi sayesinde, daha hassas ölçümler yapılabilecek ve daha uzak mesafelere veri transferi gerçekleştirilebilecektir. 6G teknolojisi ile birlikte, hücrelerin Tbps seviyelerinde işlem hacmine çıkması beklenmektedir. Bu nedenle, THz telsiz haberleşmenin hücre ana bağlantılarında etkin bir rol üstlenmesi, daha yüksek veri hızlarına ulaşılmasını ve daha fazla cihazın bağlanmasını mümkün kılacaktır. Bunun yanı sıra, veri merkezlerinde kabinetler arası iletişim ve veri transferinin THz dalgaları ile gerçekleştirilmesi, kablolama maliyetinin düşürülmesini sağlayacak ve merkezin dizaynında esneklik sağlayacaktır. Bu da veri merkezlerinin daha etkin bir şekilde yönetilmesine yardımcı olacaktır. THz teknolojisi, özellikle yüksek frekanslı dalgaların kullanılmasından kaynaklanan engelleri aşarak, daha yüksek veri hızlarına ulaşmayı mümkün kılan bir teknolojidir. Bu nedenle, araştırmaların bu alanda devam etmesi ve yeni teknolojilerin geliştirilmesi, kablosuz iletişim teknolojileri için önemli bir alan olmaya devam edecektir.

Bununla birlikte, THz iletişim sistemlerinin uygulanması, önemli yayılma kayıpları, moleküler emilim ve anten yanlış hizalanmasının sistem performansı üzerindeki etkileri nedeniyle zorluklar ortaya çıkarmaktadır. Moleküler emilim özellikle yüksek frekanslarda sorun olarak ortaya çıkmaktadır bu yüzden THz frekanslarına bağlıdır ve farklı moleküllerin farklı emilim spektrumları vardır. Bu nedenle, THz sinyalleri, yol boyunca karşılaştığı moleküller tarafından emilim ile karşılaşır ve sinyal gücünün kaybedilmesine neden olur.

Bu yüksek lisans tezi, THz iletişim sistemlerindeki yukarıda bahsedilen zorlukları ele almayı amaçlamaktadır. Temel hedefimiz, anten hizalamasının sistem performansı üzerindeki etkilerini analiz etmektir. Bu amaçla, anten hizalamasının haberleşme kanalına olan etkisini doğru bir şekilde karakterize edebilen kapsamlı bir ölçüm sistemi tasarladık ve uyguladık. Kapsamlı deneyler ve ölçümler yaparak, anten hizalamasının neden olduğu sistem performansının bozulmasını nicelendirmeyi ve temel mekanizmaları ayrıntılı bir şekilde anlamayı hedefliyoruz. Ayrıca, özellikle THz iletişim sistemleri için özelleştirilmiş yeni gelişmiş varış açısı (AoA) tahmin teknikleri geliştirmeyi amaçlıyoruz. Bu teknikler, ileri sinyal işleme algoritmaları ve yenilikçi anten dizaynlarından faydalanarak, hizalama sorunu olsa bile gelen sinyallerin varış açılarını doğru bir şekilde tahmin etmeyi sağlayacaktır. AoA tahmininin doğruluğunu artırarak, THz sistemi tasarımının hüzme oluşturma, uzaysal çoğullama ve diğer önemli yönlerinde önemli ilerlemelerin kaydedilmesini bekliyoruz.

Araştırma çabalarımız aracılığıyla, gelecek nesiller için daha verimli ve güvenilir THz kablosuz iletişim sistemlerinin gelişimine katkıda bulunmayı hedefliyoruz. Anten hizalamasının etkisini azaltarak ve AoA tahmininin doğruluğunu artırarak, daha yüksek veri hızlarına, geliştirilmiş kapsamaya ve genel sistem performansına sahip THz sistemlerinin mümkün olacağını düşünüyoruz. Bu çalışma, kablosuz iletişime katkı sağlayabilir ve 6G ağları, ultra hızlı kablosuz bağlantılar ve yüksek kapasiteli iletişim sistemleri de dahil olmak üzere çeşitli uygulamalara THz teknolojisinin sorunsuz entegrasyonunun yolunu açabilir.

Ayrıca bu yüksek lisans tezi, mobil ağlardaki veri kapasitesinin artan talebi karşısında kablosuz iletişim sistemleri için THz bandının potansiyelini incelemektedir. Çalışma, mm-Dalga sistemler gibi geleneksel frekans spektrumlarının sınırlamalarını vurgulamakta ve THz bandının bu sınırlamaları nasıl aşabileceğini göstermektedir. THz kablosuz iletişim sistemlerinde AoA tahmini ve anten hizalamasının ele alınması için kapsamlı ölçüm kampanyaları ve yeni algoritmaların önemi vurgulanmaktadır. Tez, özellikle THz tabanlı uzay bilgi ağları (SINs) için tasarlanmış olan ve hesaplama açısından verimli olmasının yanı sıra AoA tahminini doğru bir şekilde gerçekleştirebilen yeni bir algoritma olan AoSA-gold-MUSIC'i önermektedir. Ölçüm kampanyasından elde edilen kanal darbe ve frekans yanıtlarının analizi, elektromanyetik dalgaların farklı senaryolardaki davranışı hakkında değerli bilgiler sunmakta ve THz bandının bozucu ölçütlere sahip gelecek nesil kablosuz iletişim sistemlerinin yolunu açabileceğini göstermektedir. Bu ölçütler arasında, 100 Gbps'ye kadar veri hızları, 0.1 ms gibi düşük gecikme süresi ve yüksek spektrum verimliliği yer almaktadır. Tez, THz bandı ve kablosuz iletişim sistemlerinde daha fazla araştırma ve geliştirme ihtiyacını vurgulayarak, potansiyelinin tam olarak açığa çıkarılması ve artan veri kapasitesi ve bilgi alışverişi taleplerinin karşılanması için önemini vurgulamaktadır.

Tezin 2. bölümünde, THz frekanslarında anten hizalaması ile ilgili sorunların genel bir bakışı sunulmuş ve bir potansiyel çözüm olarak AoA tahmin tekniklerinin kullanımı ele alınmıştır. THz frekanslarında anten hizalamasının önemi, özellikle THz frekanslarını kullanan insansız hava araçları (UAVs) ve SINs bağlamında vurgulanmıştır. Ayrıca, SINs'lerin THz frekanslarını kullandığı bağlamda, anten

hizalaması sorununu ele almak için AoA tahmin tekniklerinin önemi bu tezin bu bölümünde detaylı bir şekilde tartışılmıştır.

Bölüm 3'te, yanlış hizalamanın THz iletişim sistemleri üzerindeki etkisini değerlendirmek amacıyla, Gebze'deki Türkiye Bilimsel ve Teknolojik Araştırma Kurumu'nda (TÜBİTAK) bulunan MİLTAL tesisinde bir ölçüm düzeneği kurulmuştur. Kurulum, 240 GHz ile 300 GHz arasındaki frekans aralığında THz kanallarını modellemek için tasarlanmıştır. Ölçümler, 240 GHz ile 300 GHz arasında değişen frekanslar kullanılarak bir dizi mesafe ve açı boyunca gerçekleştirilmektedir. Mesafe aralıkları 10 cm'lik artışlarla 20 cm ila 100 cm arasında değişmektedir. Açı aralıkları 0° ila 30° arasındaki her mesafede, 0° ila 15° arasındaki 1° aralıklarla ve 15° ila 20° arasındaki 5° aralıklarla ölçülür. Bu kapsamlı veri seti ile elektromanyetik dalgaların çeşitli senaryolardaki davranışlarına ilişkin değerli bilgiler sağlanmaktadır. Ölçüm çalışmaları, bu frekans aralığında değişen mesafelerin ve antenin yanlış hizalanmasının kanalın kompleks kazanç üzerindeki etkisini araştırmayı amaçlamaktadır. Çalışmanın sonuçları, anten yanlış hizalamasının THz kablosuz iletişim için kritik bir faktör olduğunu ve alınan gücün hem antenler arasındaki mesafeden hem de yanlış hizalamanın derecesinden önemli ölçüde etkilendiğini göstermektedir.

Bölüm 4'te, THz kablosuz sistemlerde AoA'yı gelişmiş doğruluk ve azaltılmış karmaşıklıkla belirlemek için yeni bir yöntem tanıtılmıştır. Hem verici hem de alıcıda tekdüze düzlemsel dizi (UPA) kullanan sistemler için THz frekanslarında çalışan SIN'lerin ani hareketlerinden dolayı Doppler'in tam olarak kompanze edilemediği durumlarda ortaya çıkan artık Doppler'i hesaba katan kanal modeli analiz edilmiştir. Daha sonra, THz iletişim sistemleri için genel sistem modelini tanımlamak için alt diziler dizisi (AoSA) mimarisi kullanılır. Bu mimari, MIMO verici ve alıcılarındaki yüksek sayıda kullanılan antenden kaynaklanan donanım karmaşıklığı ve güç tüketimi problemlerine çözüm olmak için daha az sayıda RF zinciri kullanımına olanak sağlamaktadır. Son olarak, sonuçlar AoSA-gold-MUSIC algoritmasının hem doğruluk hem de hesaplama verimliliği açısından standart MUSIC algoritmasından daha iyi performans gösterdiğini ortaya koymaktadır. Ayrıca, AoSA-gold-MUSIC algoritmasının performansı farklı sinyal-gürültü oranı (SNR) değerleri ve değişen artık Doppler varyansı için değerlendirilmiştir. Bu yaklaşımın THz kablosuz iletişim sistemleri için önemli pratik etkileri olabilir.

Bu tez, kablosuz iletişim sistemleri için THz bandının potansiyelini araştırmaktadır ve özellikle mobil ağlardaki veri kapasitesinin artan talebini ele almaktadır. Geleneksel frekans spektrumlarının, örneğin mm-Dalga sistemlerinin sınırlamalarını vurgulamakta ve THz bandının bu sınırlamaları nasıl aşabileceğini göstermektedir. Tez, kapsamlı ölçüm kampanyaları ve THz kablosuz iletişim sistemlerinde doğru AoA tahmini ve anten hizalamasının ele alınması için yeni algoritmaların önemini vurgulamaktadır. Özellikle THz tabanlı SIN için özelleştirilmiş olan AoSA-gold-MUSIC adlı yeni bir algoritma önerilmektedir ve hem etkin hem de doğru AoA tahmini sunmaktadır. Kanal darbe ve frekans yanıtlarının analizi, elektromanyetik dalgaların farklı senaryolardaki davranışı hakkında değerli bilgiler sunmakta ve THz bandının gelecek nesil kablosuz iletişim sistemleri için bozucu potansiyelini göstermektedir. Tez, THz bandı ve kablosuz iletişim sistemlerinde daha fazla araştırma ve geliştirme

ihtiyacını vurgulayarak, potansiyelinin tam olarak açığa çıkarılması ve artan veri kapasitesi ve bilgi alışverişi taleplerinin karşılanması için önemini vurgulamaktadır.

1. INTRODUCTION

The potential for high-speed data transfer rates and increased spectral efficiency of THz wireless communication systems have attracted significant attention in recent years. The THz frequency range, which lies between the microwave and infrared spectrums, offers unique opportunities for a wide range of communication and sensing applications. With the growing popularity of UAVs and SINs, THz communication systems have become increasingly important for these platforms. However, realizing the full potential of THz systems in UAVs platforms and SINs requires addressing several technical challenges, including antenna misalignment and AoA estimation.

Antenna misalignment, which refers to the deviation of the actual antenna orientation from the intended direction, can have a negative impact on the performance of THz communication systems. This misalignment can cause a reduction in signal quality, increased error rates, and decreased data transfer rates. In UAVs platforms, antenna misalignment can be caused by various factors, such as changes in the orientation of the UAVs, environmental factors, and mechanical disturbances. Therefore, it is crucial to accurately quantify and correct for antenna misalignment in THz communication systems in UAVs platforms to ensure optimal performance.

AoA estimation, on the other hand, is a critical aspect of THz communication systems, especially in SINs. AoA estimation refers to the process of determining the direction-of-arrival (DoA) of a signal and can be used to improve the accuracy of channel state information (CSI), which in turn can improve the overall performance of communication systems. AoA estimation can also be used to enhance the accuracy of beamforming algorithms, which are employed to improve the SNR and reduce interference in THz systems. In SINs, the residual doppler effect is also an important factor to consider for the performance of the AoA estimation algorithms.

Fortunately, there are several approaches that can be used to mitigate the negative impact of antenna misalignment on THz communication systems, including adaptive

beamforming algorithms and self-calibration techniques. Adaptive beamforming algorithms can dynamically adjust the beam direction to compensate for misalignment using information obtained from AoA estimation algorithms. Self-calibration techniques use a feedback loop to measure the deviation of the actual antenna orientation from the intended direction and make adjustments to correct for misalignment. AoA estimation algorithms play a critical role in both of these techniques, providing the necessary information to dynamically adjust the beam direction and correct for misalignment. By utilizing these techniques, it is possible to improve the performance and reliability of THz communication systems and fully realize the potential of this exciting technology. In conclusion, the importance of addressing antenna misalignment and AoA estimation in THz communication systems, particularly in UAVs platforms and SINs, cannot be overstated. This thesis explores the impact of antenna misalignment on THz communication systems, as well as various AoA estimation techniques, with the goal of improving the performance and reliability of these systems.

1.1 Contributions

This thesis aims to address the challenge of antenna misalignment in THz communication systems and improve the performance of these systems through AoA estimation techniques.

Our contribution is threefold. First, comprehensive literature review of antenna misalignment and AoA estimation techniques for THz communication systems, with a focus on UAVs platforms and SINs in Chapter 2. In this chapter, the importance of antenna misalignment in THz frequencies is discussed, particularly in the context of UAVs. Furthermore, the chapter addresses AoA estimation techniques as a passive solution to mitigate misalignment, specifically in the context of SINs utilizing THz frequencies.

Second, the impact of misalignment on THz communication systems is examined in Chapter 3. The results of a measurement campaign are then provided as a magnitude of channel frequency and impulse responses, exploring the effect of different distances

and antenna misalignment on THz communication systems within the frequency range of 240 GHz to 300 GHz. Chapter 3 has been submitted to arXiv.

Third, a novel method is introduced for determining the AoA in THz SINs systems, which offers improved accuracy and reduced complexity in Chapter 4. The channel model for SINs, employing UPA at both the transmitter and receiver, is initially analyzed. Subsequently, the overall system model for THz communication systems is described using the architecture of AoSA. Finally, results demonstrating the superior performance of the AoSA-gold-MUSIC algorithm over the standard MUSIC algorithm are presented. Additionally, the performance of the AoSA-gold-MUSIC algorithm is evaluated under varying residual Doppler variance and different SNR values. Chapter 4 has been accepted to 2022 IEEE Future Networks World Forum (FNWF).

1.2 Outline

The remaining part of the thesis is structured as follows: In Chapter 2, a comprehensive literature review is conducted, with a specific focus on antenna misalignment and AoA estimation techniques in THz communication systems. The review gives particular attention to the utilization of UAV platforms and their significance in the context of SINs. Chapter 3 provides a detailed description of the measurement setup designed for analyzing THz channels. The chapter also presents the measurement outcomes within the same section. Chapter 4 presents a novel approach in THz SINs systems for determining the AoA with decreased complexity. The thesis concludes with a discussion of the findings and the future directions for research in this area.

2. A REVIEW ON TERAHERTZ WIRELESS COMMUNICATION SYSTEMS

In this chapter, an exhaustive state of the survey regarding THz communication systems, effect of misalignment on THz frequencies and AoA estimation techniques in THz communication systems. First, we will introduce the critical importance, advantages and disadvantages of THz communication systems for next generation wireless communication systems. Second, we will discuss the importance of antenna misalignment in THz frequencies and assess the topic in the context of UAVs that are planned to be used in these frequencies. Then, we will discuss AoA estimation techniques as a solution to the misalignment problem and address the topic in the context of SINs that are planned to use THz frequencies. According to the International Telecommunication Union (ITU), it is anticipated that by 2030, the worldwide volume of wireless data traffic will reach a staggering 5 zettabytes per month, accompanied by a potential increase in the number of interconnected devices surpassing 50 billion. As a result, industries and academia are actively exploring possibilities beyond 5G and envisioning the advent of sixth-generation (6G) networks [1]. Among the diverse and cutting-edge solutions being considered, THz communications emerges as an immensely promising technology for the era of 6G and beyond. THz communication refers to communications within the ultra-wide THz band, spanning from 0.1 to 10 THz, and presents a highly favorable opportunity to tackle the challenges of spectrum scarcity and capacity limitations encountered in 5G networks [2]. The remarkable characteristics of THz communication, such as the availability of vast bandwidths ranging from tens to hundreds of gigahertz and the utilization of exceptionally short wavelengths, hold immense potential in addressing the soaring demands of data-intensive applications. This technology is poised to enable transformative applications including holographic telepresence, extended reality, and ultra high-speed wireless backhaul. Therefore, similar to the initial vision and subsequent implementation of mm-Wave communications in 5G, THz communication

is destined to play an indispensable role in the development of 6G and the future landscape of wireless networks [3].

The utilization of the THz band, particularly carrier frequencies above 300 GHz, presents a distinct set of challenges that have not been previously encountered at sub-6 GHz or mmWave frequencies [4]. These challenges encompass various crucial aspects. Firstly, the THz band is characterized by significant spreading loss and a high level of channel sparsity. Additionally, it exhibits a unique form of molecular absorption loss, which is influenced by both the frequency of transmission and the distance covered. Moreover, the propagation of THz signals is highly susceptible to blockages due to the extremely short wavelengths involved. Even objects with small dimensions can effectively impede THz signals, leading to potential disruptions. Furthermore, the presence of substantial reflection and scattering losses results in the notable attenuation of non-line-of-sight (NLoS) rays, highlighting the need for establishing reliable line-of-sight (LoS) links [5]. Consequently, these distinct propagation phenomena in the THz band necessitate the development of innovative communication and signal processing mechanisms specifically tailored for THz communication.

2.1 Investigating the Effect of Misalignment on THz Frequencies

There will be a growing demand for faster data transmission rates to keep up with the increasing amount of communication traffic [6] as next-generation wireless communication systems evolve. THz wireless systems are expected to be a strong option for 6G and future wireless systems because of their large contiguous bandwidth and applicability to indoor and outdoor communication [7]. Furthermore, due to the lack of allocated THz bands for specific active services worldwide, there exists a significant opportunity to fulfill the demand for the required communication traffic in an extensive manner.

Along with their benefits, THz frequencies also come with high attenuation due to molecular absorption and spreading loss [8], which limits the communication range in this frequency region significantly.

Thus the more dense deployment of the THz communication systems is required. One potential solution is the usage of the UAVs [9], especially where instant high-capacity communication is required in densely populated environments. UAVs play a vital role in numerous potential wireless system applications, including serving as aerial base station (ABS). ABS deployment can significantly improve the coverage, reliability, energy efficiency, and capacity of wireless networks [10].

Thus, UAVs are expected to play a crucial role in THz-enabled communication links, which are expected to trigger also new opportunities and innovative services, thanks to their 3D positioning capabilities and cost-efficient technology [11].

However, THz-integrated UAVs bring new challenges to the field. Although the utilization of large antenna arrays with directional beamforming or highly directional antennas at both the transmitter and receiver sides has been proposed as a solution to reduce the high transmission loss in the THz frequency range, these systems require accurate beam alignment. Nevertheless, the instability of UAVs caused by wind or complex movements of UAVs, including uncontrolled tilts and rotations, makes it difficult to maintain precise beam alignment, leading to an inevitable low SNR. Thus towards 6G networks, when THz communication systems are realized, the misalignment scenarios should be investigated comprehensively in terms of analyzing and modeling their effects for the specific applications.

There have been numerous studies in the literature that analyze the effects of antenna misalignment on THz communication systems. The majority of these studies have used simulations to examine the effects of antenna misalignment analytically [12]–[15] in different environments and at different frequencies of THz. For example, [12], and [13] used simulations to examine the effects of antenna misalignment on communication systems operating at 300 GHz in a simulated office environment, considering realistic propagation conditions and different types of antennas. In [14], the performance of multicarrier THz wireless system under misalignment fading is analytically evaluated. The pointing error impairments under fog conditions are analyzed in [15].

On the other hand, there are measurement-based works that investigate the effect of the misalignment [16,17].

The researchers focused on how the distance and misalignment between the transmitter and receiver affect the received power in these systems and also evaluated the effect of a single degree of misalignment on path loss in [16]. The performance of the THz communication systems operating at different frequencies has been examined in case of antenna misalignment in the [17].

Most importantly, the authors in [18] have designed a drone-based measurement setup to investigate the effects of mobility uncertainties on mm-Wave/THz-band communications between flying drones.

Furthermore, measurement, modeling, and analysis for THz wireless channels are presented extensively in [6].

Maximizing the potential of THz communication systems requires a deep understanding of their performance in realistic scenarios. As the realization of the UAVs with the THz communication devices become increasingly prevalent, the effect of misalignment becomes prominent. Thus, gathering application-specific measurements and analyzing their impact on channel frequency response (CFR) and channel impulse response (CIR) is crucial.

While the majority of the works have been done analytically to investigate the effects of the different peculiarities, this study focuses on the impact of distance and antenna misalignments on THz communication by conducting measurements using the single sweep method. Even though there is several work has been done to investigate this effect, there are no comprehensive measurements. For this purpose, an application-specific measurement setup is used, which allows the collection of measurements. Also, considering the high bandwidth opportunity of the THz frequencies, the measurements cover the 60 GHz band between 240 GHz and 300 GHz. The collected data is then analyzed by the CFR and CIR to gain insights about the joint effect of the distance and misalignment.

2.2 Angle of Arrival Estimation for Terahertz-enabled Space Information Networks

The realization of vertical networks in combination with terrestrial networks is considered as a solution for extending wireless services to remote areas with reduced latency [19]. SINs are ideal candidates to be the backbone of such a network architecture due to their coverage and the ability to connect inter-space and vertical networks with space networks [20]. According to National Aeronautics and Space Administration (NASA)'s analysis, the growth factor of space communication networks is expected to be around 10 in 30 years [21]. Additionally, to support the increasing bandwidth requirements of future networks, new frontiers for wireless communication systems are being explored, such as communication at THz frequencies. However, THz frequencies come with the cost of molecular absorption and path loss. Since molecular absorption is eliminated in space, the propagation losses can be reduced by generating high-gain narrow beams with large antenna arrays.

Due to various hardware limitations, the traditional fully digital multiple-input multiple-output (MIMO) system cannot be used in the THz band. As a result, a cost-effective alternative, hybrid ultra massive multiple-input multiple-output (UM-MIMO), which uses a smaller number of radio frequency (RF)-chains for beamforming, is adopted [22,23]. There are three main types of hybrid MIMO architecture: the fully-connected (FC) architecture [22], the AoSA structure [24], and dynamic architectures [23], [25], [26]. Among these, the AoSA structure [24] has been shown to provide a good balance between spectral efficiency and power consumption, making the beam management techniques developed for this structure applicable to any UM-MIMO system.

This makes the THz suitable candidates for SINs communications and thousands of cross-linked low-orbit satellites can establish a mesh structure in space with tens of terabits per second capacity. Such networks also have remarkable issues to be considered; due to the high mobility of SINs and strong directivity of THz beams with

massive MIMO structure, accurate AoA estimation of the incoming signal becomes more challenging.

In order to maintain a reliable and high-capacity communication link, accurate AoA information is essential for beam alignment. As even a small misalignment of the beam can result in a significant degradation of performance and even disruptions in precise beam transmissions [27,28], it is important to ensure that the beam is properly aligned.

Additionally, such a system should be cost-effective and computationally efficient while providing high-precision AoA estimation. The utilization of an AoSA structures which allows the use of fewer RF-chains, has been proposed to reduce the hardware complexity and power consumption concerns caused by the high number of antennas on massive MIMO transceivers [29].

In this context, the application of graphene-based antennas with AoSA, which have a smaller size than traditional antennas and allow for utilization of more antennas per area with higher directivity, is becoming feasible even at THz frequencies [30]. Also, the use of massive MIMO structures brings additional computational load to existing AoA estimation algorithms.

The DoA estimation is a critical step in THz UM-MIMO communication systems. It involves determining the direction from which the signals are coming. Typically, the estimation is performed using a beamforming training (BFT) procedure, where the receiver analyzes sets of pilot symbols using different beam configurations. However, in order to maintain uninterrupted and reliable transmission, DoA tracking is also necessary to account for changes in the channel. This involves continuously monitoring the DoA and adjusting the beams accordingly. Despite its importance, DoA tracking can add extra overhead and computational complexity to the BFT procedure. Therefore, in order to take full advantage of THz UM-MIMO communication systems, it is essential to have millidegree-level DoA estimation and millisecond-level tracking. This requires precise and efficient methods for determining the DoA and tracking it over time, while taking into account the unique properties of THz beams and the acceptable transmission latency [31].

Thus, more efficient AoA estimation algorithms are required to obtain precise AoA information without loss of performance. Contemporary AoA techniques, which are classified as on-grid and off-grid, can not meet AoA estimation requirements in terms of efficiency and accuracy for THz enabled SINs. Because, on-grid methods, such as compressive sensing (CS) based techniques, compute costly sparse support vectors for AoA estimation [22]. Other on-grid schemes such as [32], [33] are highly complex. Because the accurate AoA estimation is only possible when grid resolution is increased, which brings extra search overhead. On the other hand, off-grid methods such as MUltiple SIgnal Classification (MUSIC) [34], Estimation of Signal Parameters via Rotational Invariant Techniques (ESPRIT) [35], and root-MUSIC [36] can achieve higher estimation accuracy with more reasonable computational complexity compared to on-grid methods.

However, AoSA based massive MIMO structures cannot directly take advantage of these conventional off-grid approaches because of their efficiency considerations and unique design. Thus, computationally efficient novel estimation methods should be developed which can be able to obtain precise AoA from reduced RF-chains without loss of performance in order to be used in AoSA based THz-enabled SINs.

Motivated by these issues and inspired by the work of [37], utilization of an AoA estimation method based on a AoSA structure, namely AoSA-gold-MUSIC is proposed for THz-based low-orbit SINs. The method consists of two stages and allows obtaining precise AoA information while being computationally efficient. We evaluate the performance of the proposed method for reliable beam training by addressing misalignment and propagation loss in THz-enabled SINs. More importantly, a realistic metric of residual Doppler is presented. This occurs when the Doppler cannot be accurately compensated due to instantaneous rapid motion changes of SINs operating at THz frequencies and results in AoA estimation errors. We also examine the effect of the residual Doppler on AoSA-gold-MUSIC estimation performance.

Finally, to obtain correct AoA information with an error below 1°, the required parameters for the system model, such as observation period parameters with the

number of RF-chains and antennas, are also provided to ensure a stable and robust communication link under residual Doppler effects.

2.3 Summary

In this chapter, we focus on the challenges and potential solutions for THz communication systems. THz frequencies offer a large contiguous bandwidth that can provide high-capacity communication in densely populated areas, but they also come with high attenuation due to molecular absorption and spreading loss. To overcome this, the usage of UAVs has been proposed, but accurate beam alignment is difficult due to the instability caused by wind or complex movements. Therefore, investigating the effect of misalignment is crucial for analyzing and modeling their effects for specific applications.

The majority of previous studies have used simulations to analyze the effects of antenna misalignment on THz communication systems, while others have conducted measurements to investigate this effect. We contribute to this field by conducting measurements using the single sweep method to analyze the impact of distance and antenna misalignment on THz communication. We also propose a novel AoA estimation method based on an AoSA structure for THz-enabled SINs. The proposed method allows obtaining precise AoA information while being computationally efficient and addresses the effect of residual Doppler on estimation performance.

3. INVESTIGATING THE EFFECT OF MISALIGNMENT ON TERAHERTZ FREQUENCIES

In the previous chapter, a comprehensive literature review was conducted, focusing on antenna misalignment and AoA estimation techniques in THz communication systems. The review provided valuable insights into the significance of antenna misalignment and the potential solutions offered by AoA estimation techniques.

In this chapter, we examine the impact of misalignment on THz communication systems. We present the results of our measurement campaign, which investigates the impact of varying distances and antenna misalignment at the 240 GHz to 300 GHz frequency range.

3.1 Signal Model

The effect of misalignment between transmitter and receiver is investigated for THz channels in the anechoic chamber. To simplify the analysis part, the traditional linear, time-invariant channel model approach is used. The received signal can be expressed as

$$r(t) = x(t) * h(t) + n(t), \tag{3.1}$$

where $x(t)$ is the tranmitted known pilot signal, $h(t)$ denotes the communication channel and $n(t)$ represents the noise. So, the channel at the baseband can be represented as

$$h(t) = \sum_{l=0}^{L-1} \alpha_l e^{-j2\pi f_c t_l} \delta\left(t - t_l\right), \tag{3.2}$$

where L, α_l, and t_l represent the number of multipath components, channel complex gain, and delay for the l-th path, respectively. In the context of continuous-time signals, especially for narrowband signals, channels are frequently represented as combinations of impulse-like functions, typically Dirac delta functions, multiplied by amplitude responses. These responses elucidate how the channel influences both signal amplitude and phase, with gradual changes over time. Narrowband signals are characterized by

slowly evolving amplitude and phase responses in relation to their central frequency. As a result, it is a common practice to model these responses as a summation of impulse responses. These impulse responses can be convolved with the transmitted signal to assess the channel's effects and facilitate signal recovery.

As we have mentioned before, measurements have been carried out in a fully isolated anechoic chamber, so we can assume there is only LoS signal transmission.
Thus, LoS channels can be derived for $L = 1$ (3.2) as

$$h(t) = a_f e^{j\theta} \delta(t - t_0), \tag{3.3}$$

where a_f, θ, and $t_0 = d/c$ denote the LoS path complex gain, phase of the signal, and propagation delay, respectively. Also, d is the distance between the transmitter and receiver, and c is the speed of the light.

The free-space loss in an antenna system quantifies the power difference between the transmitter's output and that of an isotropic (0 dBi) antenna positioned at the receiving location. This loss occurs because of how the transmitting antenna disperses its signal. When a transmitting antenna emits a signal, it forms a spherical wavefront, but only a fraction of this spherical wavefront is intercepted by the receiving antenna. In the case of a free-space, far-field range, it is straightforward to calculate this loss using the range transfer function.

$$FSPL_{\text{dB}} = 32.4 + 20\log f_{\text{GHz}} + 20\log d_{\text{m}} \tag{3.4}$$

where d, f and c indicate distance between transmitter and receiver, operating frequency and speed of light, respectively [38].

3.2 Measurement Setup and Methodology

In communication systems that operate at THz frequencies, a sensitive measurement setup is required due to the very short wavelength of the electromagnetic waves involved. THz waves have wavelengths in the range of 0.1 millimeters to 1 millimeter, which makes them much shorter than the radio waves used in traditional communication systems.

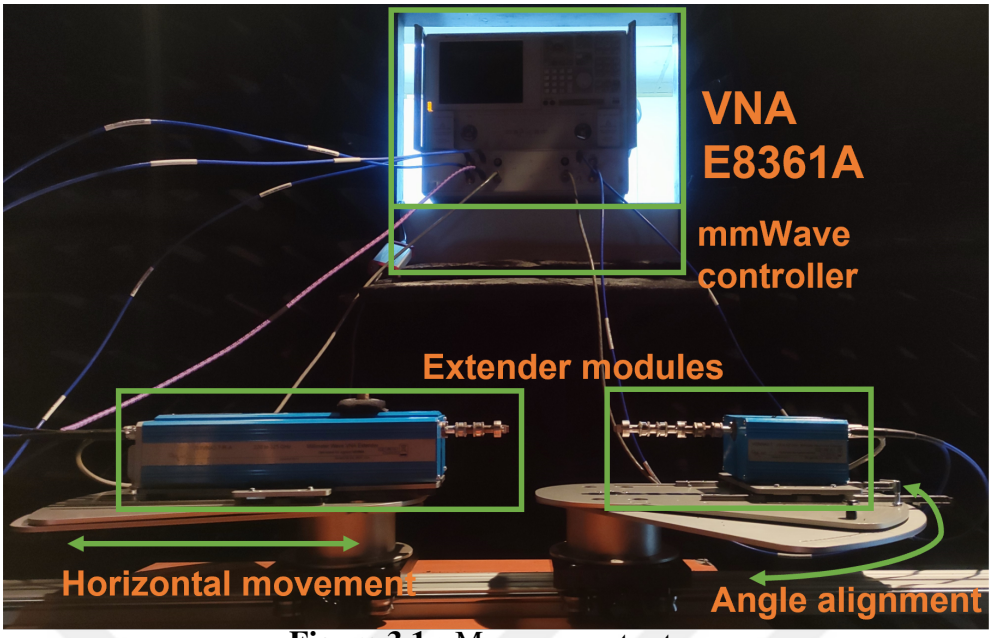

Figure 3.1 : Measurement setup

At these high frequencies, even small variations in the environment or in the components of the system can have a significant impact on the quality of the signal. Therefore, having a sensitive system is necessary to obtain accurate results. In this study, a measurement system with 1° sensitivity, which can also move in the horizontal axis, was designed at TÜBİTAK. Our THz experimental setup shown in Figure 3.1 is constructed in the MİLTAL at the TÜBİTAK. The measurement setup consists of four main hardware parts and mechanical parts. The mechanical structure consists of two sliding platforms positioned opposite to each other and a linear guide rail. The rail allows for adjusting the distance between the THz receiver and transmitter while maintaining their alignment. Furthermore, there is a mechanism on the platforms for precise angle adjustment at 1° intervals. This enables reliable measurements to be taken in both perfectly aligned and controlled misalignment scenarios. Figure 3.2 shows a three-dimensional (3D) model depicting the mechanical components of the measurement setup. Because of the low beamwidth at high frequencies such as THz, the alignment between the transmitter and receiver needs to be very precise. So, the extender modules have been installed in a mechanical system where we can precisely change the distance and angles between the modules.

Hardware parts of the system are Agilent vector network analyzer (VNA) E8361A, Oleson Microwave Labs (OML) V03VNA2-T and V03VNA2–T/R–A millimeter wave

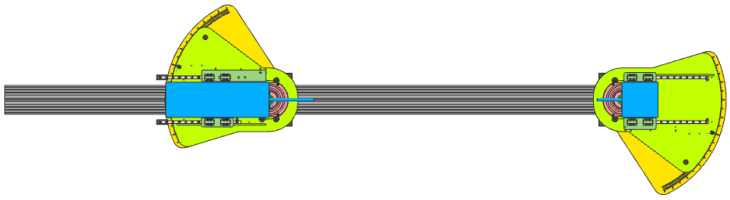

(a)

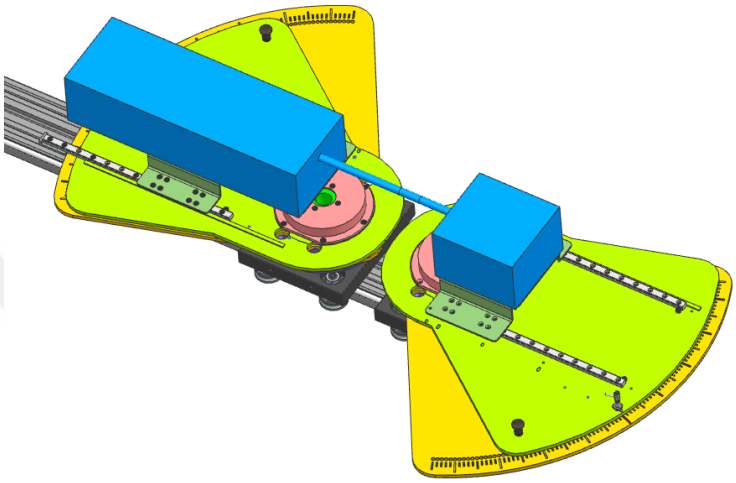

(b)

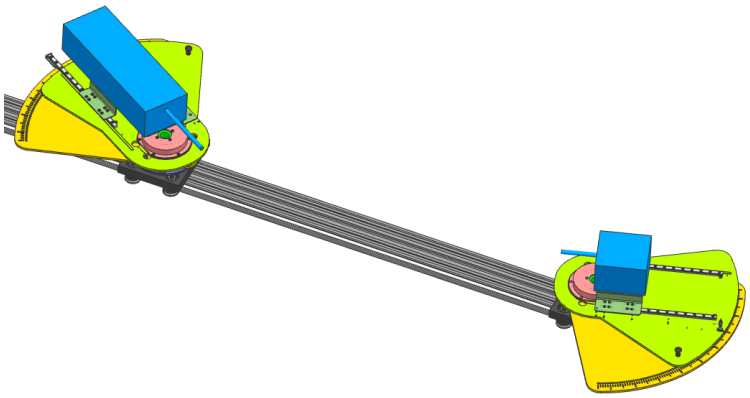

(c)

Figure 3.2 : A three-dimensional (3D) model depicting the mechanical components of the measurement setup.

extender modules and N5260A extender controller [39]. We coupled the extender modules, which work between 220 GHz and 325 GHz, to the VNA to analyze the

misalignment impact at the THz frequency band due to the VNA's 67 GHz frequency limit. V03VNA2–T/R–A multiplies the input RF signal between 12.2 GHz and 18.1 GHz with 18 in order to extend the 220 GHz to 325 GHz frequency range. Prior to signal transmission, the test intermediate frequency (IF) and reference IF signals for a VNA are acquired through the process of downconversion using mixers. After that received signal passing through the channel is downconverted at the V03VNA2–T, and the resulting test IF signal is fed back to the VNA.

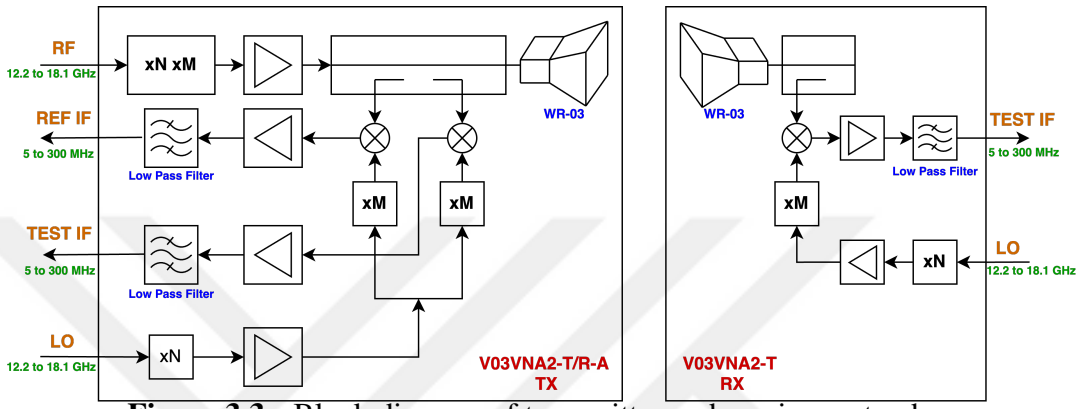

Figure 3.3 : Block diagram of transmitter and receiver extenders

Figure 3.3 provides a detailed block diagram of the measurement setup, along with the up-conversion and down-conversion operations that are carried out on the extenders.

The source modules have been driven by an extended band WR-10 multiplier chain with a WR-03 waveguide output interface. The WR-03 waveguide output power of the V03VNA2-T/R-A is around -23dBm. The extender characteristics are as follows; the phase stability is $\pm$0.4dB in the range of $\pm 8^{\circ}$, typical dynamic range is 75dB with the minimum of 60dB [40]. Two Elmika-branded components are incorporated in a series to the RF ports of the extenders for measurement purposes. The first component is a WR-3 (220GHz-325GHz) waveguide, which is directly attached to the RF port of the extender. The second component is a WR-3 horn antenna, which is directly mounted at the end of the waveguide. Also, horn antennas have a gain of 24.8dBi at their center frequency.

The operating frequency range is set to 240 GHz to 300 GHz because the magnitude and phase stability of the extender modules has better performance in this range. Before measuring the s-parameters, we calibrated the extender modules by connecting

Table 3.1 : Measurement parameters

Description	Value
Operating frequency	240 GHz - 300 GHz
Bandwidth	60 GHz
Measurement frequency points	4096
IF bandwidth	100 Hz
Spectral resolution	14.648 MHz
Antenna misalignment	0° : 1° : 15° and 15° : 5° : 30°
Distance (cm)	20:10:100 cm

the transmitter and the receiver module's waveguide ports for realible channel characteristics results. The process of calibration starts by first removing the WR-3 antennas at the ends of the two extenders and connecting the extenders to each other by joining both wave-guides. This creates a direct connection between the two extenders via the wave-guides. The calibration process is then initiated through the software that manages the VNA. The Figure 3.4 displays the end-to-end connection between the transmitter and receiver during the calibration. The results of the calibration are compensated and saved as complex S_{21} parameters for each measurement point.

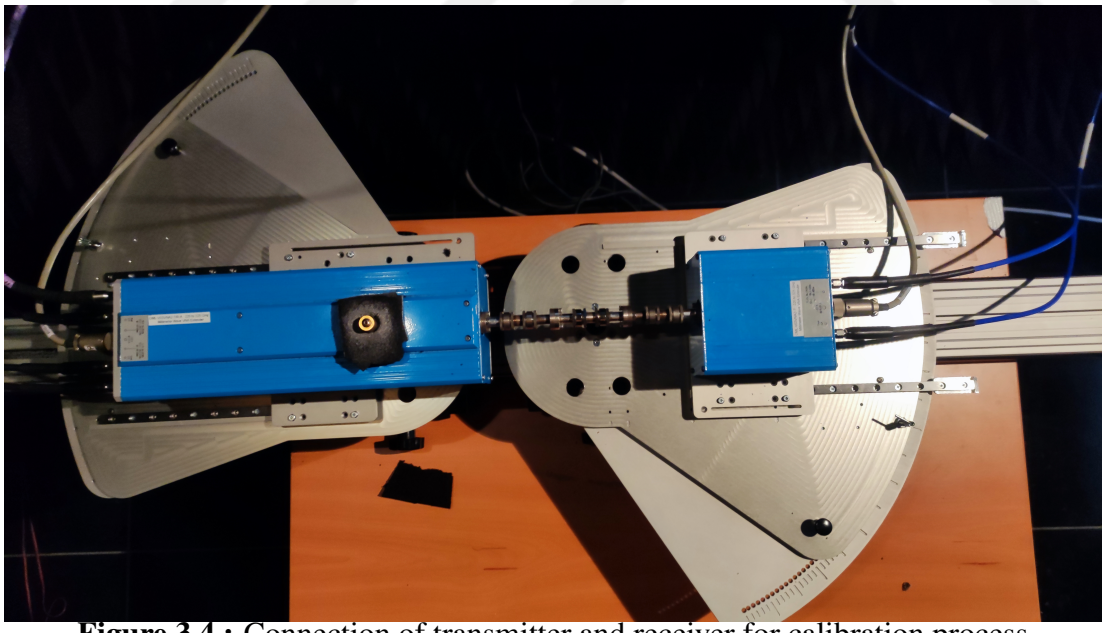

Figure 3.4 : Connection of transmitter and receiver for calibration process

Following calibration, 4096 points with an IF bandwidth of 100 Hz are used to measure the 60 GHz band.

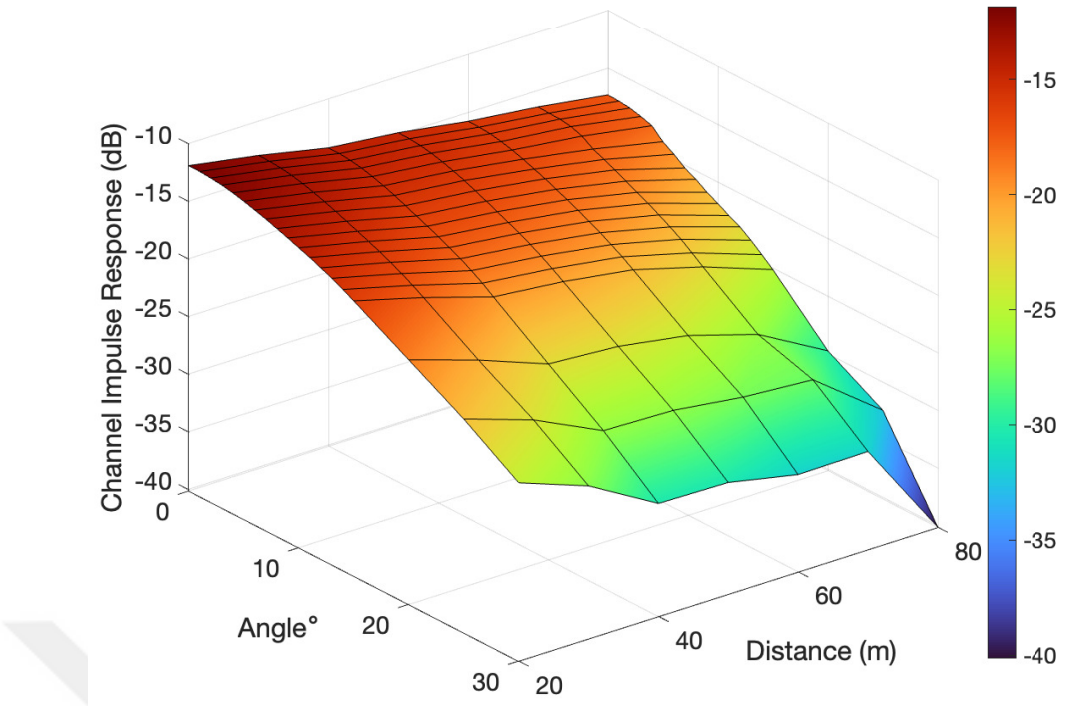

Figure 3.5 : Maximum values of the channel impulse response for all distances and antenna misalignment degress

The 240 GHz to 300 GHz frequency range is measured using OML extenders equipped with standard gain horn antennas. The spectral resolution is set at 14.648 MHz as each spectral measurement is associated with 4096 frequency points. The measurement system comprises calibrated connectors and cables, ensuring accurate measurements. To analyze the effect of distance and antenna misalignment in the THz wireless channel, measurements were taken with the help of the rail and angle alignment system, which allows elevational angle change with the precision of 1° at each distance setting. Meanwhile, the position and angle of the receiver module were changed by keeping the receiver fixed. For the sake of simplicity, only horizontal antenna misalignment is considered. For each case, the parameter S_{21} parameters are stored as complex numbers in Agilent VNA E8361A.

3.3 Measurement Results

In this section, we delve into the measurement results of our THz communication system, with a particular focus on the joint impact of antenna misalignment and distance-dependent signal loss. Notably, we encountered inconsistencies in our

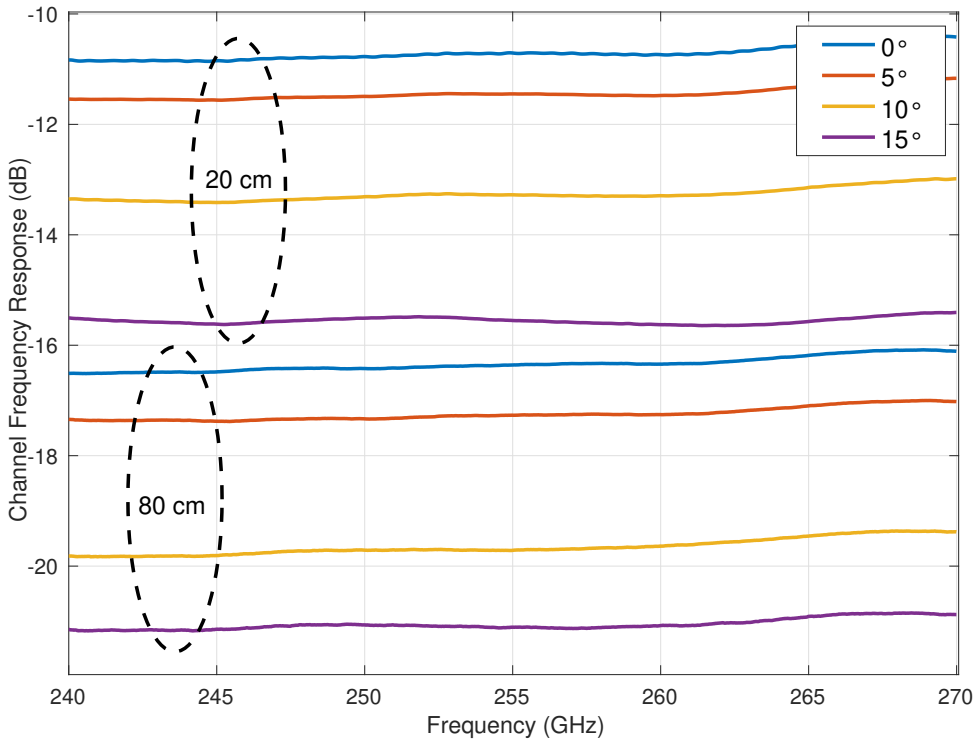

Figure 3.6 : Magnitude of the channel frequency response with $0°, 5°, 10°$ and $15°$ antenna misalignment at 20 cm and 80 cm distances

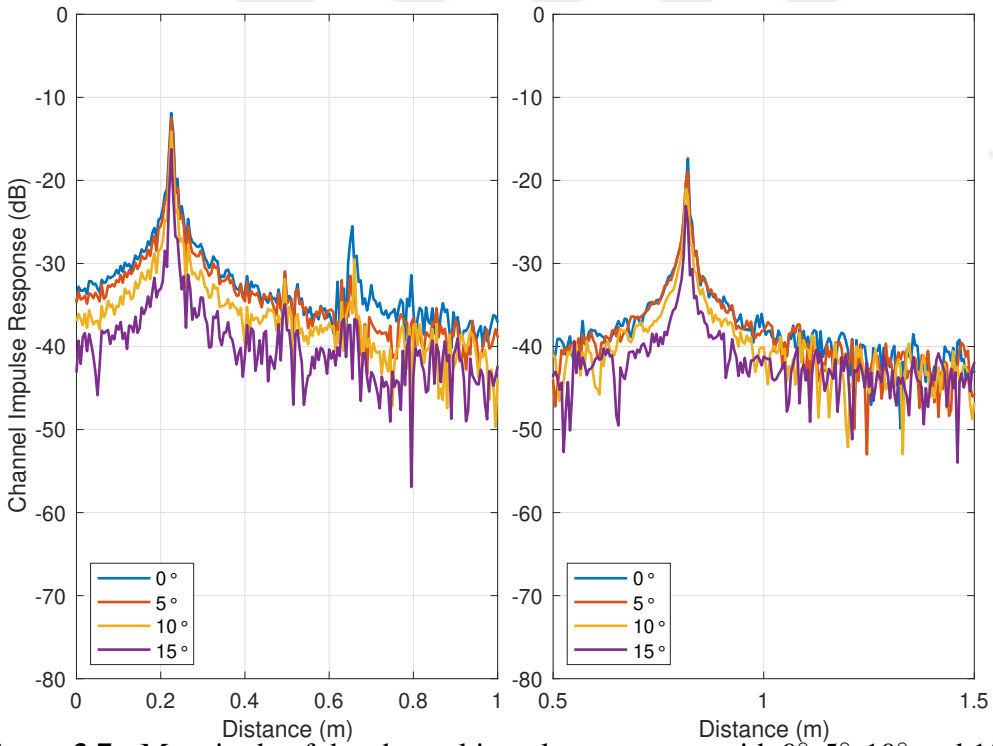

Figure 3.7 : Magnitude of the channel impulse responses with $0°, 5°, 10°$ and $15°$ antenna misalignment at 20 cm and 80 cm distances

measurements between the frequency range of 270 GHz and 300 GHz, which could be attributed to various factors such as the sensitivity of our measurement equipment

to the THz frequency range, environmental conditions, and inherent uncertainties in THz signal propagation. So, the measured values beyond 270 GHz have not been included in the simulation results. Recognizing these limitations is crucial for the accurate interpretation of our results.

The magnitude of channel complex gains, as depicted in Figure 3.6, reveals the substantial influence of antenna misalignment and distance on the THz channel. Increasing misalignment angles result in a pronounced reduction in signal strength, a phenomenon exacerbated by the narrow beamwidth characteristic of THz antennas, underscoring the critical importance of precise alignment for optimal system performance.

Furthermore, our time-domain analysis, illustrated in Figure 3.7 through an inverse Fourier transform (FT) of measurement data, provides deeper insights into how antenna misalignment affects the channel. When we examine the x-axis, the left figure represents a channel impulse response where there is a 20cm distance between the transmitter and receiver. On the other hand, in the right figure, the channel impulse response shows a significantly longer distance of 80cm between the transmitter and receiver. This analysis unveils signal dispersion and temporal variations, essential for system design and synchronization strategies. Examining the CIR in Figure 3.5, which combines distance and antenna misalignment measurements, allows us to discern dominant channel response characteristics by considering maximum CIR values for different distance and angle combinations. In addition, the direct numerical value equivalents of these measurement pairs are given in the Table 3.2. This information is invaluable for designing adaptive modulation and coding schemes to mitigate the combined effects of distance and misalignment.

Antenna misalignment is an indispensable concern for THz communication systems in UAV, as it has a direct impact on the received power. The distance between the transmitter and the receiver plays a crucial role in path loss, which inevitably results in a decline in the received power. In addition, when the transmitter and receiver antennas are misaligned, the issue of power loss is exacerbated, causing a further decrease in the received power. In this context, the development of fast and robust

Table 3.2 : Magnitude of the channel impulse responses at all distances and antenna misalignments

	0°	5°	10°	15°	20°	25°	30°
20 cm	-11.88	-12.51	-14.09	-16.24	-18.89	-21.56	-24.64
30 cm	-12.93	-13.67	-15.47	-17.89	-20.85	-23.58	-26.85
40 cm	-14.21	-15.03	-17.01	-19.76	-23.12	-26.45	-30.31
50 cm	-14.83	-15.69	-17.70	-20.37	-23.53	-26.62	-30.42
60 cm	-15.77	-16.60	-18.58	-21.28	-24.52	-27.41	-31.67
70 cm	-16.46	-17.66	-19.91	-22.96	-26.36	-27.84	-31.60
80 cm	-17.35	-18.96	-21.86	-25.13	-29.72	-32.42	-40.10

beamforming and beam tracking algorithms is imperative for UAVs equipped with THz communication systems. The compensation for both distance and misalignment is necessary to maintain the desired level of received power, thus ensuring reliable communication in UAVs operating with THz systems.

3.4 Conclusion

The increasing need for high data rates and the growing number of wireless devices has led to substantial interest in employing THz communication systems as a possible solution. In this pursuit, UAVs have emerged as a promising solution to address various challenges posed by modern communication needs. Nonetheless, within the promising potential of THz communication via UAVs, it becomes evident that one critical factor demands our utmost consideration: the effects of misalignment.

Effective communication in THz systems via UAVs depends on the precise alignment between transmitting and receiving antennas. This alignment serves as the cornerstone of reliable, high-quality communication. Even minor deviations from the optimal alignment can yield substantial impacts on signal quality and overall system performance. Recognizing this, it becomes imperative to address and understand the implications of misalignment thoroughly.

Our study sought to evaluate the repercussions of varying distances and levels of antenna misalignment within the challenging THz frequency range of 240 GHz to 300 GHz. We conducted these measurements in a controlled environment, an

anechoic chamber, to isolate and assess these factors systematically. The results were illuminating, underscoring the considerable influence that both distance and antenna misalignment exert on THz communication systems. These findings unambiguously emphasize the non-negotiable importance of precise alignment for optimal system operation.

While previous research has explored LOS and NLOS channels in the domain of THz communication, the challenges introduced by misalignment remain relatively uncharted territory, especially in the context of UAV-assisted systems. Consequently, there exists an evident research gap demanding our attention—a comprehensive understanding of the effects of misalignment in these dynamically evolving scenarios.

In anticipation of addressing the challenges posed by misalignment, our forthcoming chapter will introduce an innovative solution: an AoA estimation algorithm. This algorithm promises to offer a pragmatic approach to mitigating the impact of misalignment, balancing both low complexity and high accuracy. It is imperative to recognize that while this algorithm presents a valuable tool, achieving and maintaining proper alignment between antennas will remain an overarching consideration for reliable and efficient THz communication.

In conclusion, our study of THz communication alongside UAVs uncovers a landscape full of possibilities and difficulties. Misalignment poses a major challenge, and our research highlights its significant influence. As we explore the uncharted realm of UAV-supported THz communication, the AoA estimation algorithm offers a promising way to improve the reliability of these systems. However, it's important to remember that achieving and maintaining proper alignment is a key factor for the success of THz communication systems.

4. ANGLE OF ARRIVAL ESTIMATION FOR TERAHERTZ-ENABLED SPACE INFORMATION NETWORKS

After highlighting the significance and impact of antenna misalignment in THz communication systems through a measurement-based analysis in the previous chapter, we introduce a new method for determining the AoA in THz SINs systems with improved accuracy and reduced complexity in this chapter. The channel model for SINs, where both the transmitter and receiver use UPA, is analyzed. The overall system model for THz communication systems is then described using the AoSA architecture. Finally, results that demonstrate that the AoSA-gold-MUSIC algorithm outperforms the standard MUSIC algorithm in terms of computational efficiency are given. Additionally, the performance of the AoSA-gold-MUSIC algorithm is evaluated for varying residual Doppler variance and different SNR values.

4.1 System and Channel Model

In this section, first, we examine the channel model in the context of the SINs where both transmitter and receiver are equipped by $N_x \times N_z$ UPA antenna elements in the $x-z$ plane, as shown in Figure 4.1. Then, the overall system model for THz communication systems constructed by AoSA architecture is described. In this chapter, we consider the sampled signals and hence our signal model becomes discrete.

The channel matrix $\mathbf{H}$ for the THz massive MIMO can be expressed as

$$\mathbf{H} = \alpha e^{j2\pi\varepsilon} \mathbf{a}_{RX}\left(\theta_{rx}, \phi_{rx}\right) \mathbf{a}_{TX}\left(\theta_{tx}, \phi_{tx}\right)^{\mathrm{H}}, \tag{4.1}$$

where α denotes complex path gain and ε represents residual Doppler, which occurs when the Doppler cannot be fully compensated for due to the high mobility and instant movements of SINs operating at high frequencies [41,42]. Also, θ denotes the azimuth angle defined between the y axis and the signal's projection on the x-y plane, and ϕ denotes the elevation angle defined between the signal and the x-y plane $\mathbf{a}_{RX}\left(\theta_{rx}, \phi_{rx}\right)$ and transmitter $\mathbf{a}_{TX}\left(\theta_{tx}, \phi_{tx}\right)$, respectively. Since we consider the same UPA elements

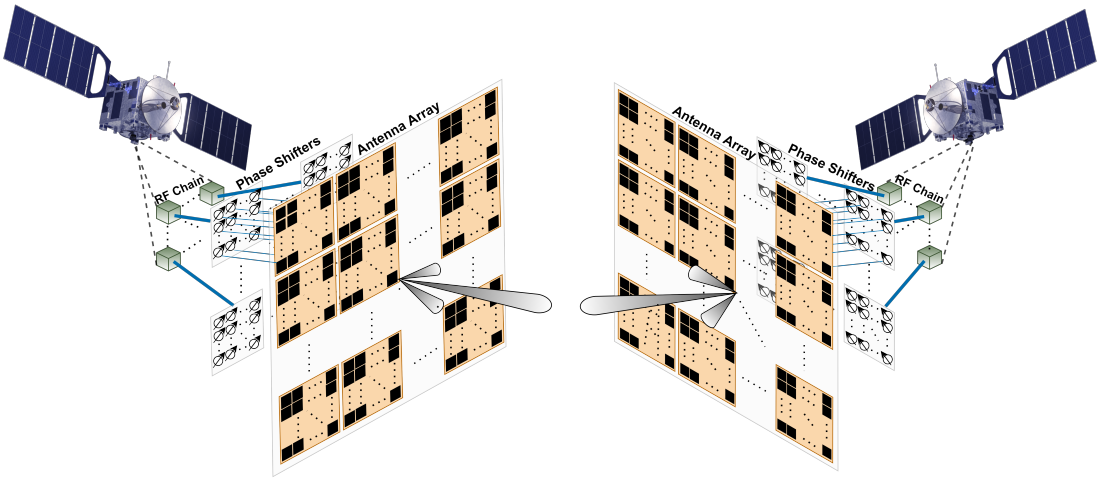

Figure 4.1 : The system architecture of the AoSA massive MIMO enabled SINs operating at THz frequencies.

for both the transmitter and the receiver, the array steering vectors can be expressed as [43]

$$\mathbf{a}(\theta,\phi) = \frac{1}{\sqrt{N_x N_z}}\Big[1,\ldots,\mathrm{e}^{j2\pi d(n_x \sin\theta\cos\phi + n_z\sin\phi)/\lambda} \ldots,\mathrm{e}^{j2\pi d((N_x-1)\sin\theta\cos\phi+(N_z-1)\sin\phi)/\lambda}\Big]^{\mathrm{T}}, \tag{4.2}$$

where $n_x = 1,2,3,...,N_x-1$ and $n_z = 1,2,3,...,N_z-1$ represent the index of the anntena elements in the UPA. Also, λ and $d = \lambda/2$ denotes the wavelength and antenna spacing, respectively. For simplicity, we can assume there is only a LoS communication link between SINs in this study since directional beams can be generated with massive MIMO and THz signals also, there are few reflection components in space.

Overall system structure with AoSA is shown in Figure 4.1. The antenna array consists of a total $N_A = N_x \times N_z$ antennas and which are connected to a number of N_{RF} RF-chains where $N_{RF} << N_A$. The one RF-chain also corresponds to a subarray in the antenna array, thus each subarray consists of $N_S = N_A/N_{RF}$ antennas [44]. Also, it is assumed that codewords are used in the signal transmission. The received signal for the c^{th} codeword can be written as

$$\mathbf{Y}_c = \mathbf{W}^{\mathrm{H}}\mathbf{H}\mathbf{F}_c\mathbf{P} + \mathbf{W}^{\mathrm{H}}\mathbf{n}, \tag{4.3}$$

where $n \sim \mathscr{CN}(0,\sigma_n^2)$ each element of the complex additive white Gaussian noise (AWGN), $\mathbf{F}_c \in \mathbb{C}^{N_A \times N_{RF}}$, and $\mathbf{W} \in \mathbb{C}^{N_A \times N_{RF}}$ denote analog precoding and combining matrices, respectively. These two matrices are being used to update the values of the

phase shifters in the transmitter and receiver during the beamforming process. Used in AoA estimation, $\mathbf{P} \in \mathbb{C}^{N_{RF} \times N_P}$ is the transmitted pilot symbol matrix with N_p pilot transmission instants and the columns of the $\mathbf{P}$ orthonormal to each other [45].

Algorithm 1 Generate Pilot Symbol Matrix

1: **function** GENERATESYMBOLMATRIX(N_P)
2: Create a complex vector which is length of N_P
3: Apply QR decomposition to complex vector which is created in Step 2.
4: $\mathbf{R} \leftarrow \text{diag}(\text{diag}(\mathbf{R})/\text{abs}(\text{diag}(\mathbf{R})))$
5: $\mathbf{P} \leftarrow \mathbf{Q} \times \mathbf{R}$
6: **end function**

$\mathbf{P}$ can be generated by the pseudocode given in Algorithm 1 where the orthonormal basis is obtained by using QR decomposition of the complex vector of N_P length. We multiply $\mathbf{Y}_c$ with $\mathbf{P^H}$ and the result can be obtained as

$$\begin{aligned} \mathbf{Y}^c &= \mathbf{W}^{\mathrm{H}}\mathbf{H}\mathbf{F}^c\mathbf{P}\mathbf{P}^{\mathrm{H}} + \mathbf{W}^{\mathrm{H}}\mathbf{n}\mathbf{P}^{\mathrm{H}}, \\ &= \mathbf{W}^{\mathrm{H}}\mathbf{H}\mathbf{F}^c + \mathbf{N}^c, \end{aligned} \tag{4.4}$$

where $\mathbf{N}^c = \mathbf{W}^{\mathrm{H}}\mathbf{n}\mathbf{P}^{\mathrm{H}} \in \mathbb{C}^{N_{RF} \times N_{RF}}$.

Since it is assumed that the pilot symbols used in the transmitter are known by the receiver, the pilot symbol matrix is used as the match filter on the receiver side [46]. As a result, the collected signal at the RF-chains for a total of C codewords can be expressed as

$$\mathbf{Y} = \mathbf{W}^{\mathrm{H}}\mathbf{a}_{RX}\alpha e^{j2\pi\varepsilon}\mathbf{a}_{TX}^{\mathrm{H}}\mathbf{F} + \mathbf{N}, \tag{4.5}$$

where $\mathbf{Y} \in \mathbb{C}^{N_{RF} \times N_{RF}C}$ and $\mathbf{N} \in \mathbb{C}^{N_{RF} \times N_{RF}C}$ denotes collected noise matrix.

4.2 AoSA Based GOLD-MUSIC for AoA Estimation

In this section, firstly, the processing steps of the received signals by utilizing the AoSA scheme for AoA estimation are described. Then, the estimation process of the AoA with gold-MUSIC is given.

Initially, it is assumed that signals of T observations are collected at the receiver, and AoA estimation is done by these acquired signals. For the processing of the acquired signals in the system, T combining matrices $\mathbf{W}$ are stacked together to obtain the radio

power in all directions. The combining matrix for the subarrays is given by

$$\mathbf{W}_{(j-1)N_S+1:jN_S,(t-1)T+j} = \frac{1}{\sqrt{N_A}} \times \mathbf{u}, \tag{4.6}$$

where $j = 1,2,3,...,N_{RF}$ and $t = 1,2,3,...,T$ represent the index of the $\mathbf{W}$. Also $\mathbf{u}$ stores phase shifter values of the each antenna element in one subarray and it is given as

$$\mathbf{u} = \left[e^{j2\pi\omega_1}, \quad e^{j2\pi\omega_2}, \quad \cdots \quad , e^{j2\pi\omega_{N_S}}\right], \tag{4.7}$$

where $\omega_{i,...,N_s}$ indicates the phase shift coefficient which is generated randomly by the $\omega \sim \mathscr{U}(0,1)$. It is used to generate different beams [47]. Also, the $\mathbf{F}$ and $\mathbf{W}$ have identical forms; the only difference is that the $\mathbf{F}$ is constructed on the transmitter side by the codewords, which store randomly generated phase shifter values, similar to the (4.7), while $\mathbf{W}$ is constructed on the receiver side by the codewords. As a result, the $\mathbf{F}$ can be denoted in the same way as in (4.6) with (4.7) [48].

Considering the $\mathbf{W}$, $\mathbf{F}$ as denoted in (4.6) and the channel matrix in (4.1), the t^{th} observation at the j^{th} RF-chain can be stated as

$$\mathbf{y}_{j,t} = \mathbf{W}^{\mathrm{H}}_{(j-1)N_S+1:jN_S,j,t}\mathbf{a}_{RX_{(j-1)N_S+1:jN_S,j}} \times \alpha e^{j2\pi\varepsilon}\mathbf{a}^{\mathrm{H}}_{TX}\mathbf{F} + \mathbf{N}_{j,t}. \tag{4.8}$$

After the T observations, total observation matrix for the j^{th} RF-chain with the concatenation of $\{\mathbf{y}_{j,t}\}_{t=1}^{T}$ can be represented as

$$\overline{\mathbf{Y}}_j = \left[\mathbf{y}^{\mathrm{T}}_{j,1}, \ldots, \mathbf{y}^{\mathrm{T}}_{j,T}\right]^{\mathrm{T}} = \overline{\mathbf{B}}_j \alpha e^{j2\pi\varepsilon}\mathbf{a}^{\mathrm{H}}_{TX}\mathbf{F} + \overline{\mathbf{N}}_j \tag{4.9}$$

where $\overline{\mathbf{Y}}_j \in \mathbb{C}^{T\times N_s C}$, and $\overline{\mathbf{N}}_j = \left[\mathbf{N}_{j,1}, \ldots, \mathbf{N}_{j,T}\right]^{\mathrm{T}} \in \mathbb{C}^{T\times N_s C}$ with

$$\overline{\mathbf{B}}_j = \begin{bmatrix} \left(\mathbf{W}^{\mathrm{H}}_{(j-1)N_S+1:jN_S,j,1}\mathbf{a}_{RX_{(j-1)N_S+1:jN_S,j}}\right)^{\mathrm{T}}, \ldots \\ \ldots, \left(\mathbf{W}^{\mathrm{H}}_{(j-1)N_S+1:jN_S,j,t}\mathbf{a}_{RX_{(j-1)N_S+1:jN_S,j}}\right)^{\mathrm{T}} \end{bmatrix}^{\mathrm{T}} \tag{4.10}$$

where $\overline{\mathbf{B}}_j \in \mathbb{C}^{T\times 1}$. Finally, we can represent all observations for all RF-chains in the AoSA structure with the combination of $\{\overline{\mathbf{Y}}_j\}_{j=1}^{N_{RF}}$ as below

$$\tilde{\mathbf{Y}} = \left[\overline{\mathbf{Y}}^{\mathrm{T}}_1, \ldots, \overline{\mathbf{Y}}^{\mathrm{T}}_{N_{\mathrm{RF}}}\right]^{\mathrm{T}} = \tilde{\mathbf{B}}\alpha e^{j2\pi\varepsilon}\mathbf{a}^{\mathrm{H}}_{TX}\mathbf{F} + \tilde{\mathbf{N}}. \tag{4.11}$$

In order to estimate AoA from the observed signal in (4.11) with the MUSIC algorithm, the covariance matrix of $\tilde{\mathbf{Y}}$ is calculated as follows

$$\mathbf{R}_{\mathrm{y}} = \frac{1}{N_{\mathrm{RF}}}\tilde{\mathbf{Y}}\tilde{\mathbf{Y}}^{\mathrm{H}}. \tag{4.12}$$

Then, to reveal the signal and the noise subspaces, the eigenvalue decomposition is applied to the $\mathbf{R}_{\mathrm{y}}$ and it can be expressed as

$$\mathbf{R}_{\mathrm{y}} = \mathbf{U}_{\mathrm{s}}\mathbf{\Sigma}_{\mathrm{s}}\mathbf{U}_{\mathrm{s}}^{\mathrm{H}} + \mathbf{U}_{\mathrm{n}}\mathbf{\Sigma}_{\mathrm{n}}\mathbf{U}_{\mathrm{n}}^{\mathrm{H}} \tag{4.13}$$

where $\mathbf{\Sigma}_{\mathrm{s}} \in \mathbb{C}^{1\times 1}$ contains eigenvalues of the signal subspace and $\mathbf{\Sigma}_{\mathrm{n}} \in \mathbb{C}^{(N_{\mathrm{RF}}T-1)\times(N_{\mathrm{RF}}T-1)}$ contains eigenvalues of the noise subspace. Also, $\mathbf{U}_{\mathrm{s}} \in \mathbb{C}^{N_{\mathrm{RF}}T\times 1}$ denotes the corresponding eigenvectors of the signal subspace, and similarly $\mathbf{U}_{\mathrm{n}} \in \mathbb{C}^{(N_{\mathrm{RF}}T-1)\times(N_{\mathrm{RF}}T-1)}$ denotes the corresponding eigenvectors of the noise subspace. The AoA estimation can be obtained by exploiting the orthogonality between signal and noise subspaces.

Algorithm 2 AoSAGoldMUSIC

1: **function** AoSAGoldMUSIC($Y, searchAngles, W, T$)
2: Calculate covariance matrix of $\tilde{\mathbf{Y}}$ using Eq. 4.12
3: Apply eigenvalue decomposition to the covariance matrix in order to get noise and signal eigenvectors.
4: Create the low-resolution angle pairs matrix of binary combinations of each θ and ϕ angle to fully scan the angle space.
5: **for** $s \leftarrow 1, \text{length}(anglePairs)$ **do**
6: $\mathbf{a_{RX}} \leftarrow \text{generateSteeringVectors}(anglePairs(s))$
7: Create the $\mathbf{B}$ vector according to Eq. 4.10
8: **for** $k \leftarrow 1, N_{RF}$ **do**
9: Create the $\mathbf{s}(\theta,\phi)$ vector in Eq. 4.14.
10: **end for**
11: Create the pseudo spectrum vector using (4.16)
12: **end for**
13: Find the peak point in the pseudo spectrum.
14: Repeat lines 4-11 with higher resolution around the pre-estimated AoA to estimate a finer AoA.
15: **end function**

To be able to do this, the array steering vector $\mathbf{s}(\theta,\phi)$, which scans all elevation and the azimuth angles of the received signal, is generated as follows

$$\mathbf{s}(\theta,\phi) = \begin{bmatrix} \mathbf{W}^{\mathrm{H}}_{(j-1)N_S+1:jN_S,j,1}\mathbf{a}_{RX_{(j-1)N_S+1:jN_S,j}}, \cdots \\ \cdots, \mathbf{W}^{\mathrm{H}}_{(j-1)N_S+1:jN_S,j,T}\mathbf{a}_{RX_{(j-1)N_S+1:jN_S,j}} \end{bmatrix}. \tag{4.14}$$

When the values scanned by the array steering vector coincide with the direction of the incoming signal, the following holds true, $\mathbf{s}^{\mathrm{H}}(\theta,\phi)\mathbf{U}_{\mathrm{n}} = 0$ and the AoA can be estimated with

$$(\theta,\phi)_{\mathrm{MUSIC}} = \operatorname{argmin} \mathbf{s}^{\mathrm{H}}(\theta,\phi)\mathrm{U}_{\mathrm{n}}\mathrm{U}_{\mathrm{n}}^{\mathrm{H}}\mathbf{s}(\theta,\phi). \tag{4.15}$$

Table 4.1 : Simulation parameters of Figure 4.2 for RMSE comparison

Notations	Description	Value
f_c	Carrier frequency	300 GHz
N_A	Number of antennas at Tx and Rx	1024
N_{RF}	Number of RF chains at Tx and Rx	$4, 8, 16$
ϕ and θ	Azimuth and elevation angles at Tx and Rx	$\mathscr{U}(-90, 90)$
T	Observation time	$4, 8, 16$
ε	Residual Doppler	$\mathscr{U}(-0.5, 0.5)$
N_P	Length of the pilot symbol vector	N_{RF}

However, to obtain spectral peaks, AoA can be represented with the pseudo spectrum function as follows

$$\mathbf{P}(\theta,\phi) = \frac{1}{\mathbf{s}^{\mathrm{H}}(\theta,\phi)\mathbf{U}_{\mathrm{n}}\mathbf{U}_{\mathrm{n}}^{\mathrm{H}}\mathbf{s}(\theta,\phi)}. \tag{4.16}$$

Because of the high speeds of the satellites, the AoA should be estimated quickly in order to maintain a continuous communication link. Due to the fact that the array steering vector in (4.14) is directly proportional to the number of antennas, the size of the $\mathbf{s}(\theta,\phi)$ can be large in massive MIMO systems. As a result, scanning the entire angular spectrum using a high-resolution array steering vector in the MUSIC algorithm increases the estimation load. Instead, the gold-MUSIC algorithm, which is a two-stage scanning method, initially uses the low-resolution array steering vector to discover the spectral region roughly where the true AoA is located. Then, it can provide a sharper and faster estimation of AoA by utilizing a higher resolution array steering vector by scanning the pre-estimated spectral area. Thus, in this study, we adopted the gold-MUSIC algorithm for the AoSA structure, and the pseudocode of gold-MUSIC run in context of the particular system proposed is given in Algorithm 2.

4.3 Simulation Results

In this section, the error performance of the proposed AoSA gold-MUSIC algorithm for SIN is analyzed with a Monte Carlo simulations for different parameters.

We considered a scenario where two SIN communicate with each other through LoS transmission at the center frequency of 300 GHz. The number of antennas for both transmitter and receiver are set to be $N_A = 1024$. The number of RF chains is evaluated

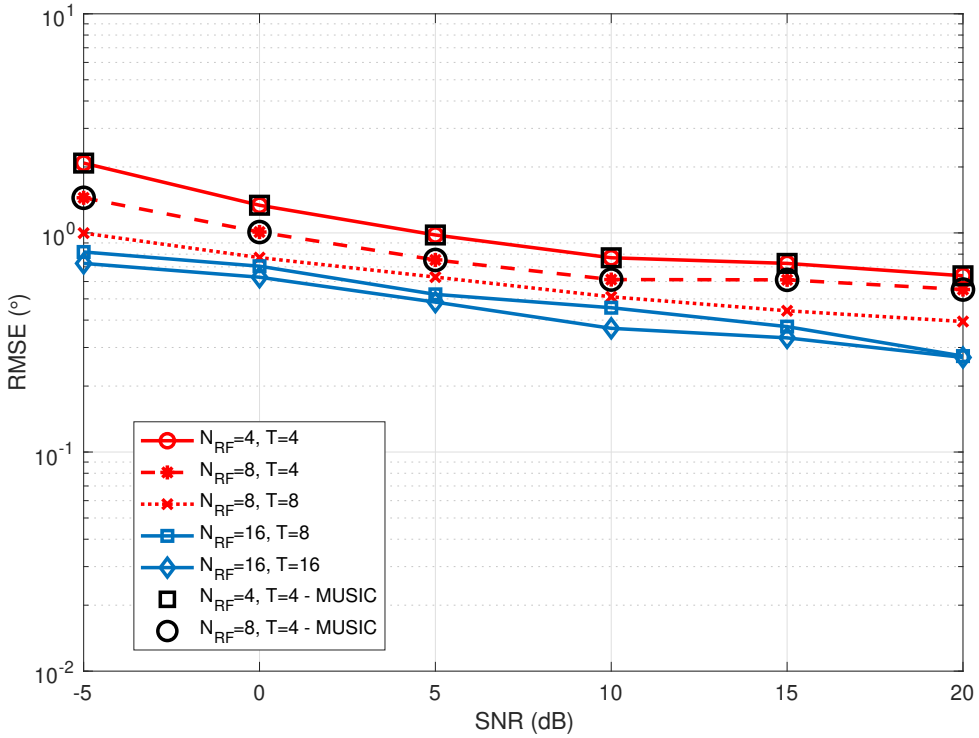

Figure 4.2 : RMSE performance of the proposed method and traditional MUSIC algorithm for the SIN for different N_{RF} and T where the residual Doppler variance is set as 0.08.

as $N_{RF} = 4, 8, 12$. Also, azimuth and elevation angles are generated randomly from $\mathscr{U}(-90, 90)$. In addition, ε is assumed to follow the uniform distribution and generated randomly from $\mathscr{U}(-0.5, 0.5)$ [42].

The simulation parameters for Figure 4.2 and Figure 4.3 are summarized in Table 4.1.

According to the simulation parameters given in Table 4.1, the AoA estimation error performance based on the AoSA gold-MUSIC with the residual Doppler is investigated in Figure 4.2. The variance of the ε is set as 0.08. It is shown that the AoSA gold-MUSIC has almost identical performance compared to the MUSIC algorithm. Also, the root mean square error (RMSE) performance of the AoSA gold-MUSIC for various residual Doppler levels with varying SNR values is shown in Figure 4.3. The RMSE formula can be expressed as

$$RMSE = \sqrt{\mathbf{E}\left[\left(\hat{\theta} - \theta\right)^2 + \left(\hat{\phi} - \phi\right)^2\right]}, \tag{4.17}$$

where $\hat{\theta}$ and $\hat{\phi}$ are the estimated elevation and azimuth angle, respectively. Also, unit of the RMSE is degree.

The parameters for this analysis are set to be $N_{RF} = 16$ and $T = 8$. It is observed that the AoA estimation error for SIN remained below 1° for all SNR values.

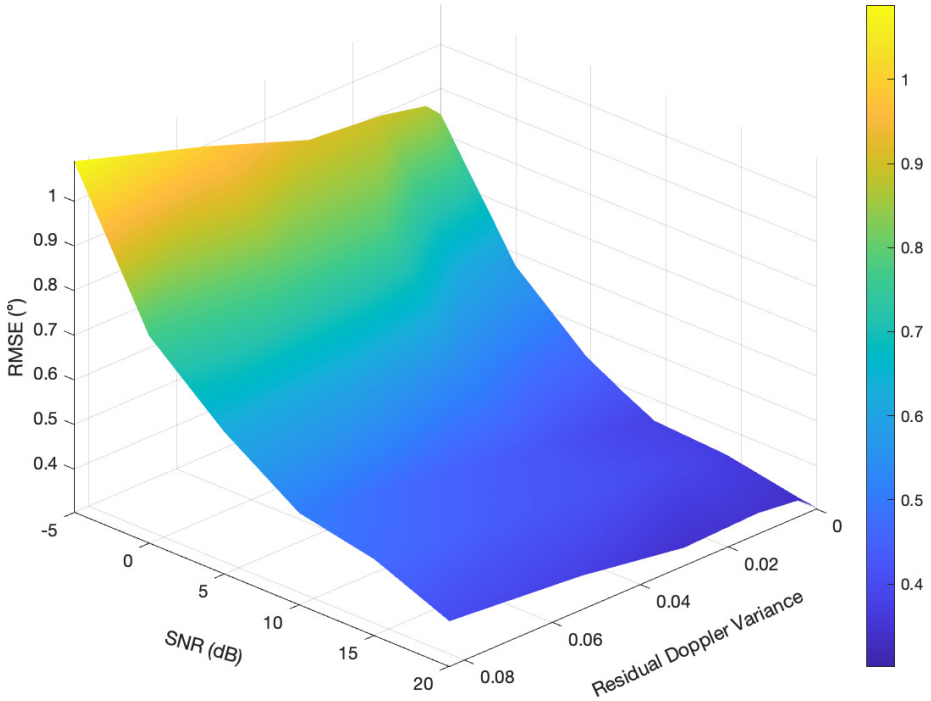

Figure 4.3 : Effect of the SNR and the residual Doppler to the RMSE

The overall computational complexity of the MUSIC and can be given as $\mathcal{O}((N_{RF}T)^3 + (N_{RF})^2 \times \frac{180}{R_A})$, where $R_A = 0.01^\circ$ denotes the grid resolution of the array steering vector. The first term $\mathcal{O}((N_{RF}T)^3)$ in MUSIC algorithm complexity analysis, comes from eigenvalue decomposition of covariance matrix and second term $\mathcal{O}((N_{RF})^2 \times \frac{180}{R_A})$ comes from scanning the angular spectrum with the given resolution. In the gold-MUSIC algorithm computational complexity reduced to $\mathcal{O}((N_{RF}T)^3)$. As a result, AoSA-gold-MUSIC can provide precise AoA information for THz enabled SINs while it is computatioally efficient compared to the MUSIC algorithm.

4.4 Conclusion

In the previous chapter, we conducted a measurement-based analysis to examine the impact of antenna misalignment on received power in THz communication systems. The results revealed that even small misalignment angles, on the order of a few degrees, can cause a significant effect on channel complex gains. This problem can be particularly critical in mobile platforms like UAVs, where maintaining

precise alignment becomes more challenging due to various motion dynamics. Therefore, ensuring accurate antenna alignment is of utmost importance to maintain the performance and reliability of THz communication systems in such mobile scenarios.

In this chapter, firstly, we addressed the importance of accurate estimation of the AoA in the massive MIMO enabled SINs operating at THz frequencies. In addition to this, we introduced the residual Doppler effect, which can lead to significant AoA inaccuracies in the practical scenarios of THz enabled SINs. Furthermore, to have a low-hardware complexity with a cost-efficient framework for the massive MIMO we considered AoSA structure for the THz enabled SINs. In this direction, we proposed the AoSA-gold-MUSIC algorithm based on AoSA structure to estimate AoA accurately in THz enabled SIN with reduced complexity. We demonstrated that the proposed AoSA-gold-MUSIC can estimate the AoA with high accuracy while being computationally efficient compared to the MUSIC algorithm. We also provided AoA estimation performance of the AoSA gold MUSIC algorithm under varying residual Doppler variance for different SNR values.

5. CONCLUSION AND FUTURE DIRECTIONS

With the exponential growth in demand for data capacity in mobile communication networks, the predicted data capacity requirements for the future are expected to reach several terabits per second (Tbps). However, conventional frequency spectrums such as the mm-Wave systems used in fifth-generation (5G) cellular networks offer limited available bandwidth, making it difficult to support such high data capacity requirements. To address this challenge, researchers are exploring new frequency spectrums, such as the THz band, which is considered the most promising candidate to overcome these limitations. Preliminary studies are underway to enable wireless communication in the THz band, which has the potential to achieve Tbps data rates and support disruptive metrics in wireless communication systems.

The THz band offers a wider bandwidth and has emerged as a promising candidate to overcome the spectrum scarcity constraint in wireless communication systems. With the potential to support data rates of Tbps, the THz band could be a key requirement for future communication systems. While preliminary studies are being conducted to enable its usage, the THz band remains largely unexplored in the realm of wireless communication systems. However, delving into the THz frequency range in wireless communication systems offers numerous opportunities for new services and innovative applications.

In particular, THz-empowered UAVs could play a significant role in enabling the deployment of sixth-generation (6G) networks. With the potential for enormous connectivity density of more than 10 million devices per 1 km^2, improved energy efficiency, and high data transmission reliability, the THz band could pave the way for a new era of wireless communication systems with disruptive metrics. These potential benefits encompass achieving data rates ranging from 10 to 100 Gbps, achieving end-to-end latency below 0.1 ms, attaining microsecond-level jitter performance, achieving a spectrum efficiency of 100 bps/Hz, ensuring 99.99999% reliability in data

transmission, and achieving millimeter-level resolution and accuracy for positioning and sensing purposes. As such, the exploration of the THz band in wireless communication systems is of great interest to researchers and industry experts alike, as it could potentially transform the way we communicate and exchange information in the future. However, to enable wireless communication in the THz band and explore its potential for novel applications, such as on mobile platforms like UAVs and satellites, there is a need to conduct comprehensive measurement campaigns and develop new algorithms specifically designed for this frequency range.

In order to enable wireless communication in the THz band and explore its potential for novel applications on mobile platforms like UAVs and satellites, it is necessary to conduct comprehensive measurement campaigns that address the challenges of antenna misalignment due to platform movements. To mitigate the effects of antenna misalignment, new algorithms should be developed to estimate the AoA, specifically designed for this frequency range. This could include beamforming techniques, which have been shown to be a promising candidate solution for the problem of antenna misalignment. Therefore, conducting measurement campaigns and developing new algorithms for AoA estimation and beamforming are critical steps towards enabling the usage of the THz band in wireless communication systems.

This thesis has highlighted the challenges of THz wireless communication, including the importance of accurate estimation of AoA in massive MIMO enabled systems operating at THz frequencies and the essential role of antenna alignment in THz wireless communication. To address these challenges, a wide measurement campaign was organized within the scope of this thesis, and a measurement setup was designed at TÜBİTAK to take measurements at various distances and angles in the 240-300 GHz range. The measurement setup was used to collect data at 10 cm intervals ranging from 20 cm to 100 cm distances, and from 0 degrees to 30 degrees. The analysis of the channel impulse and frequency responses from these measurements revealed that the channel complex gains varies not only with the distance between transmitter and receiver but also with frequency. Additionally, the findings from the measurement campaign and analysis highlight the need for developing new algorithms, such as AoA estimation and beamforming techniques, to mitigate the effects of antenna

misalignment in THz wireless communication systems. To address these challenges, this work proposed a new AoSA-gold-MUSIC algorithm based on the AoSA for THz enabled SINs with reduced complexity. The proposed algorithm accurately estimates AoA while being computationally efficient, with higher accuracy compared to the MUSIC algorithm. By addressing these challenges and investing in further research and development, the full potential of the THz band can be unlocked, leading to a new era of wireless communication systems that meet the ever-increasing demand for data capacity and exchange of information.

Overall, this thesis has laid the groundwork for further research and development in the THz band and wireless communication systems in 6G networks, providing valuable insights into the challenges and potential solutions for achieving high-speed, reliable, and energy-efficient communication.

REFERENCES

[1] **Saad, W.**, **Bennis, M. and Chen, M.** (2019). A vision of 6G wireless systems: Applications, trends, technologies, and open research problems, *IEEE network*, *34*(3), 134–142.

[2] **Huq, K.M.S.**, **Busari, S.A.**, **Rodriguez, J.**, **Frascolla, V.**, **Bazzi, W. and Sicker, D.C.** (2019). Terahertz-enabled wireless system for beyond-5G ultra-fast networks: A brief survey, *IEEE network*, *33*(4), 89–95.

[3] **Akyildiz, I.F.**, **Han, C. and Nie, S.** (2018). Combating the distance problem in the millimeter wave and terahertz frequency bands, *IEEE Communications Magazine*, *56*(6), 102–108.

[4] **Elayan, H.**, **Amin, O.**, **Shihada, B.**, **Shubair, R.M. and Alouini, M.S.** (2019). Terahertz band: The last piece of RF spectrum puzzle for communication systems, *IEEE Open Journal of the Communications Society*, *1*, 1–32.

[5] **Shafie, A.**, **Yang, N.**, **Han, C.**, **Jornet, J.M.**, **Juntti, M. and Kurner, T.** (2022). Terahertz communications for 6G and beyond wireless networks: Challenges, key advancements, and opportunities, *IEEE Network*.

[6] **Han, C.**, **Wang, Y.**, **Li, Y.**, **Chen, Y.**, **Abbasi, N.A.**, **Kürner, T. and Molisch, A.F.** (2022). Terahertz wireless channels: A holistic survey on measurement, modeling, and analysis, *IEEE Communications Surveys & Tutorials*, *24*(3), 1670–1707.

[7] **Boulogeorgos, A.A.A.**, **Alexiou, A.**, **Merkle, T.**, **Schubert, C.**, **Elschner, R.**, **Katsiotis, A.**, **Stavrianos, P.**, **Kritharidis, D.**, **Chartsias, P.K.**, **Kokkoniemi, J.** *et al.* (2018). Terahertz technologies to deliver optical network quality of experience in wireless systems beyond 5G, *IEEE Communications Magazine*, *56*(6), 144–151.

[8] **Jornet, J.M. and Akyildiz, I.F.** (2011). Channel modeling and capacity analysis for electromagnetic wireless nanonetworks in the terahertz band, *IEEE Transactions on Wireless Communications*, *10*(10), 3211–3221.

[9] **Azari, M.M.**, **Solanki, S.**, **Chatzinotas, S. and Bennis, M.** (2022). THz-empowered UAVs in 6G: Opportunities, challenges, and trade-offs, *IEEE Communications Magazine*, *60*(5), 24–30.

[10] **Giordani, M.**, **Polese, M.**, **Mezzavilla, M.**, **Rangan, S. and Zorzi, M.** (2020). Toward 6G networks: Use cases and technologies, *IEEE Communications Magazine*, *58*(3), 55–61.

[11] **Azari, M.M.**, **Solanki, S.**, **Chatzinotas, S.**, **Kodheli, O.**, **Sallouha, H.**, **Colpaert, A.**, **Montoya, J.F.M.**, **Pollin, S.**, **Haqiqatnejad, A.**, **Mostaani, A.** *et al.* (2022). Evolution of non-terrestrial networks from 5G to 6G: A survey, *IEEE communications surveys & tutorials*.

[12] **Priebe, S.**, **Jacob, M. and Kürner, T.** (2012). The impact of antenna directivities on THz indoor channel characteristics, *2012 6th European Conference on Antennas and Propagation (EUCAP)*, IEEE, pp.478–482.

[13] **Priebe, S.**, **Jacob, M. and Kürner, T.** (2012). Affection of THz indoor communication links by antenna misalignment, *2012 6th European Conference on Antennas and Propagation (EUCAP)*, IEEE, pp.483–487.

[14] **Papasotiriou, E.N.**, **Boulogeorgos, A.A.A. and Alexiou, A.** (2020). Performance analysis of THz wireless systems in the presence of antenna misalignment and phase noise, *IEEE Communications Letters*, *24*(6), 1211–1215.

[15] **Badarneh, O.S.** (2022). Performance Analysis of Terahertz Communications in Random Fog Conditions With Misalignment, *IEEE Wireless Communications Letters*, *11*(5), 962–966.

[16] **Ekti, A.R.**, **Boyaci, A.**, **Alparslan, A.**, **Ünal, İ.**, **Yarkan, S.**, **Görçin, A.**, **Arslan, H. and Uysal, M.** (2017). Statistical modeling of propagation channels for terahertz band, *2017 IEEE Conference on Standards for Communications and Networking (CSCN)*, IEEE, pp.275–280.

[17] **Sheikh, F.**, **Zantah, Y.**, **Al-Hasan, M.**, **Mabrouk, I.**, **Zarifeh, N. and Kaiser, T.** (2021). Horn Antenna Misalignments at 100, 300, 400, and 500 GHz in Close Proximity Communications, *2021 IEEE International Symposium on Antennas and Propagation and USNC-URSI Radio Science Meeting (APS/URSI)*, IEEE, pp.449–450.

[18] **Guan, Z. and Kulkarni, T.** (2019). On the effects of mobility uncertainties on wireless communications between flying drones in the mmWave/THz bands, *IEEE INFOCOM 2019-IEEE Conference on Computer Communications Workshops (INFOCOM WKSHPS)*, IEEE, pp.768–773.

[19] **Kurt, G.K.**, **Khoshkholgh, M.G.**, **Alfattani, S.**, **Ibrahim, A.**, **Darwish, T.S.**, **Alam, M.S.**, **Yanikomeroglu, H. and Yongacoglu, A.** (2021). A vision and framework for the high altitude platform station (HAPS) networks of the future, *IEEE Communications Surveys & Tutorials*, *23*(2), 729–779.

[20] **Zhang, Z.**, **Xiao, Y.**, **Ma, Z.**, **Xiao, M.**, **Ding, Z.**, **Lei, X.**, **Karagiannidis, G.K. and Fan, P.** (2019). 6G wireless networks: Vision, requirements, architecture, and key technologies, *IEEE Vehicular Technology Magazine*, *14*(3), 28–41.

[21] **Son, I.K. and Mao, S.** (2017). A survey of free space optical networks, *Digital Communications and Networks*, *3*(2), 67–77.

[22] **Méndez-Rial, R.**, **Rusu, C.**, **González-Prelcic, N.**, **Alkhateeb, A. and Heath, R.W.** (2016). Hybrid MIMO architectures for millimeter wave communications: Phase Shifters or Switches?, *IEEE Access*, *4*, 247–267.

[23] **Yan, L.**, **Han, C. and Yuan, J.** (2020). A dynamic array-of-subarrays architecture and hybrid precoding algorithms for terahertz wireless communications, *IEEE Journal on Selected Areas in Communications*, *38*(9), 2041–2056.

[24] **Lin, C.**, **Li, G.Y. and Wang, L.** (2017). Subarray-based coordinated beamforming training for mmWave and sub-THz communications, *IEEE Journal on Selected Areas in Communications*, *35*(9), 2115–2126.

[25] **Zhang, D.**, **Wang, Y.**, **Li, X. and Xiang, W.** (2017). Hybridly connected structure for hybrid beamforming in mmWave massive MIMO systems, *IEEE Transactions on Communications*, *66*(2), 662–674.

[26] **Park, S.**, **Alkhateeb, A. and Heath, R.W.** (2017). Dynamic subarrays for hybrid precoding in wideband mmWave MIMO systems, *IEEE Transactions on Wireless communications*, *16*(5), 2907–2920.

[27] **Fan, D.**, **Gao, F.**, **Liu, Y.**, **Deng, Y.**, **Wang, G.**, **Zhong, Z. and Nallanathan, A.** (2018). Angle domain channel estimation in hybrid millimeter wave massive MIMO systems, *IEEE Transactions on Wireless Communications*, *17*(12), 8165–8179.

[28] **Han, C. and Akyildiz, I.F.** (2016). Three-dimensional end-to-end modeling and analysis for graphene-enabled terahertz band communications, *IEEE Transactions on Vehicular Technology*, *66*(7), 5626–5634.

[29] **Lin, C. and Li, G.Y.L.** (2016). Terahertz communications: An array-of-subarrays solution, *IEEE Communications Magazine*, *54*(12), 124–131.

[30] **Tekbıyık, K.**, **Ekti, A.R.**, **Karabulut Kurt, G. and Görçin, A.** (2019). Terahertz band communication systems: Challenges, novelties and standardization efforts, *Physical Communication*, *35*, 100700.

[31] **Peng, B. and Kürner, T.** (2016). Three-dimensional angle of arrival estimation in dynamic indoor terahertz channels using a forward–backward algorithm, *IEEE Transactions on Vehicular Technology*, *66*(5), 3798–3811.

[32] **Marzi, Z.**, **Ramasamy, D. and Madhow, U.** (2016). Compressive channel estimation and tracking for large arrays in mm-wave picocells, *IEEE Journal of Selected Topics in Signal Processing*, *10*(3), 514–527.

[33] **Zhao, J.**, **Gao, F.**, **Jia, W.**, **Zhang, S.**, **Jin, S. and Lin, H.** (2017). Angle domain hybrid precoding and channel tracking for millimeter wave massive MIMO systems, *IEEE Transactions on Wireless Communications*, *16*(10), 6868–6880.

[34] **Guo, Z.**, **Wang, X. and Heng, W.** (2017). Millimeter-wave channel estimation based on 2-D beamspace MUSIC method, *IEEE transactions on wireless communications*, *16*(8), 5384–5394.

[35] **Liao, A.**, **Gao, Z.**, **Wu, Y.**, **Wang, H. and Alouini, M.S.** (2017). 2D unitary ESPRIT based super-resolution channel estimation for millimeter-wave massive MIMO with hybrid precoding, *IEEE Access*, *5*, 24747–24757.

[36] **Shu, F.**, **Qin, Y.**, **Liu, T.**, **Gui, L.**, **Zhang, Y.**, **Li, J. and Han, Z.** (2018). Low-complexity and high-resolution DOA estimation for hybrid analog and digital massive MIMO receive array, *IEEE Transactions on Communications*, *66*(6), 2487–2501.

[37] **Rangarao, K.V. and Venkatanarasimhan, S.** (2012). gold-MUSIC: A variation on MUSIC to accurately determine peaks of the spectrum, *IEEE Transactions on Antennas and Propagation*, *61*(4), 2263–2268.

[38] **Friis, H.T.** (1946). A note on a simple transmission formula, *Proceedings of the IRE*, *34*(5), 254–256.

[39] **Agilent**. *Agilent PNA Microwave Network Analyzers*, `https://www.omlinc.com/images/pdf/Library/Application_Notes/Agilent5989-4098_PNA_Banded_MMW_with_PSG.pdf`.

[40] **OML**. *V03VNA2 Series WR03 Frequency Extension Modules 220 to 325 GHz*, `https://www.omlinc.com/images/pdf/VxxVNA2/OML-V03VNA2_Datasheet.pdf`.

[41] **Kaushal, H. and Kaddoum, G.** (2016). Optical communication in space: Challenges and mitigation techniques, *IEEE Communications Surveys & Tutorials*, *19*(1), 57–96.

[42] **Şenyuva, R.V. and Karabulut Kurt, G.** (2021). Harmonic retrieval of CFO and frame misalignment for OFDM-based inter-satellite links, *International Symposium on Wireless Communication Systems (ISWCS)*, pp.1–5.

[43] **Chen, Y.**, **Yan, L. and Han, C.** (2020). Millidegree-level direction-of-arrival (DoA) estimation and tracking for terahertz wireless communications, *Annual IEEE International Conference on Sensing, Communication, and Networking (SECON)*, pp.1–9.

[44] **Huang, X.**, **Guo, Y.J. and Bunton, J.D.** (2010). A hybrid adaptive antenna array, *IEEE Transactions on Wireless Communications*, *9*(5), 1770–1779.

[45] **Gao, X.**, **Dai, L.**, **Zhang, Y.**, **Xie, T.**, **Dai, X. and Wang, Z.** (2016). Fast channel tracking for terahertz beamspace massive MIMO systems, *IEEE Transactions on Vehicular Technology*, *66*(7), 5689–5696.

[46] **Chen, Y. and Han, C.** (2020). Deep CNN-based spherical-wave channel estimation for terahertz ultra-massive MIMO systems, *2020 IEEE Global Communications Conference*, IEEE, pp.1–6.

[47] **Chen, Y.**, **Yan, L.**, **Han, C. and Tao, M.** (2021). Millidegree-level direction-of-arrival estimation and tracking for terahertz ultra-massive MIMO systems, *IEEE Transactions on Wireless Communications*, *21*(2), 869–883.

[48] **Chen, Y.**, **Yan, L. and Han, C.** (2021). Hybrid spherical- and planar-wave channel modeling and DCNN-powered estimation for terahertz ultra-massive MIMO systems, *IEEE Transactions on Communications*, *69*(10), 7063–7076.

CURRICULUM VITAE

Name SURNAME: Hasan NAYİR

EDUCATION:

- **B.Sc.:** 2020, Yıldız Technical University, Faculty of Electrical and Electronics Engineering, Electronics and Communication Engineering

PROFESSIONAL EXPERIENCE AND REWARDS:

- 2023- Machine Learning Engineer at Payten
- 2020-2023 Researcher at The Scientific and Technological Research Council of Turkey (Informatics and Information Security Research Center)
- 2022 Visiting Researcher at Texas A&M University Qatar

PUBLICATIONS, PRESENTATIONS AND PATENTS ON THE THESIS:

- **Nayir H.**, Kurt, G.K. and Görçin, A. (2022). Angle of Arrival Estimation for Terahertz-enabled Space Information Networks. *IEEE Future Networks World Forum (FNWF).*
- **Nayir H.**, Karakoca, E., Kurt, G. K., and Görçin, A. (2023). Experimental Assessment of Misalignment Effects in Terahertz Communications. *arXiv preprint arXiv:2305.13910.*